APPENDIX

Appendix -1	List of Collected Documents
Appendix -2	Record Photographs
Appendix -3	Existing Well Data
Appendix -4	MT/TEM Survey
Appendix-5	Preliminary Economic Analysis
Appendix-6	Volumetric Calculation Method
Appendix-7	Output of Meeting

Appendix -1 List of Collected Documents

Appendix-1 List of Collected Documents

No	Name	Author	Year
1	Projet pour l'evaluation des ressources geothermiques	Aquater	1981
2	Ressources geothermiques etudes effectuees par Aquater 1980 - 1982	Aquater	1982
3	Interpretation of gradient wells data – Hanle plain	Geotermica	1985
4	Geothermal exploration project Hanle-Gaggade republic of Djibouti – Hanle 1 report	Aquater	1987
5	Geothermal exploration project Hanle-Gaggade republic of Djibouti – Hanle 2 report	Aquater	1987
6	Carte geologique de la republique de Djibouti a 1:100,000 - Dikhil	ORSTOM	1987
7	Djibouti geothermal exploration project republic of Djibouti – draft final report	Aquater	1989
8	Data collection survey on geothermal development in the republic of Djibouti	JICA	2014
9	Decree 2011-029/PR/MHUEAT: procédure d'étude d'impact environnemental	Le president de la republique de Djibouti	2011
10	Projet d'évaluation des ressources géothermiques – Etude -Cadre d'Impact Environnemental et Social (ECIES) -	The World Bank/ FICHTNER	2012

Appendix -2 Record Photographs

Appendix-2 Record Photographs

ODDEG head office

Inception meeting at ODDEG head office

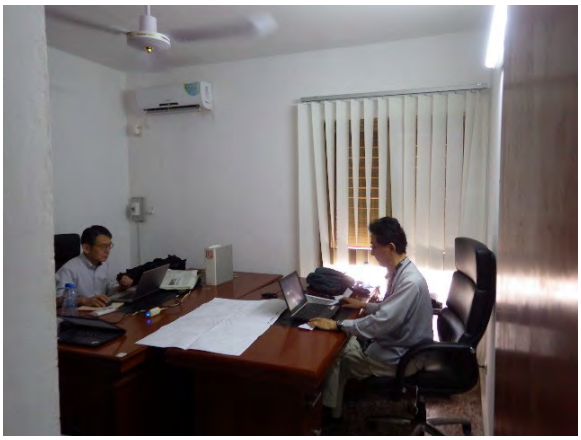

Survey team Office in ODDEG head office

Outside view of ODDEG new head office (under construction)

Inside of ODDEG new head office

MT/TEM survey: uuggage for MT/TEM survey

MT/TEM survey: unboxing/ preparation of survey equipment

MT/TEM survey: non-polarized electrode

Access road to the site

MT/TEM survey: mobilization of survey equipment at the site

MT/TEM survey: preparation of survey equipment at the site

MT/TEM survey: preparation of survey equipment at the site (batteries and data loggers)

MT/TEM Survey: preparation of induction coils

MT/TEM survey: induction coils by Phoenix

MT/TEM survey: unloading of loop coil for TEM Survey

MT/TEM survey: setting of horizontal induction coil

MT/TEM survey: setting of horizontal induction coil

MT/TEM survey: setting of vertical induction coils

MT/TEM survey: preparation for setting of non-polarized electrode

MT/TEM survey: setting of non-polarized electrode

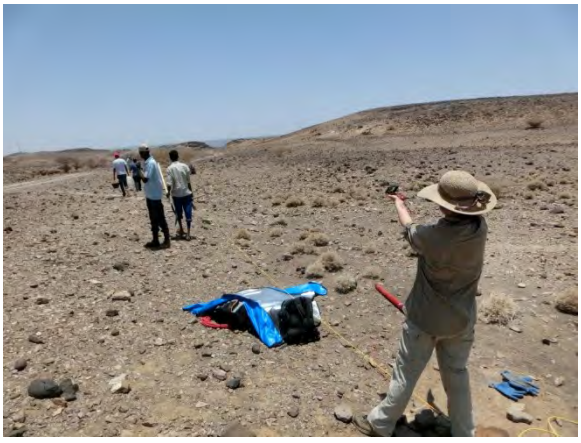

MT/TEM survey: arranging of survey equipment

MT/TEM survey: site measurement (data logger was covered by vinyl seat)

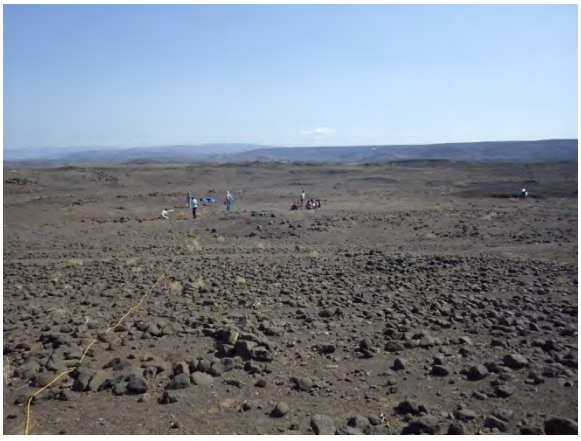

MT/TEM Survey: site measurement at the point (Center)

MT/TEM survey: data logging and analysis at the survey site

MT/TEM survey: a set of survey equipment and members

Overview of survey site: ground covered by basaltic boulders

Overview of survey site: basaltic breccias

Overview of survey site: hilly slope

Overview of survey site: some part of the surface is covered by basaltic rock.

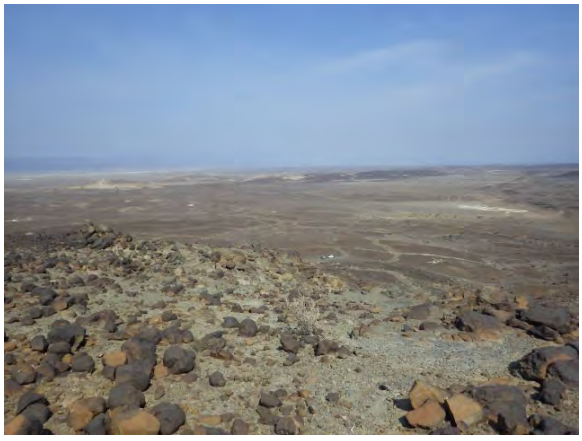

Overview of Hanle plain from survey site

Alluvial deposit in Hanle Plain

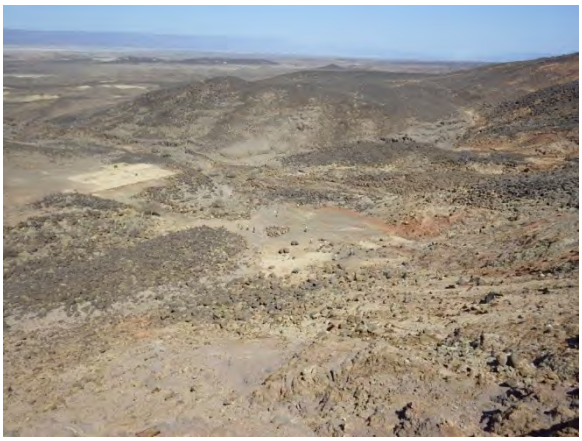

Overview of Garabbayis fumaroles and well pad

Closer view of drilling pad with existing borehole (Garabbayis-2)

Fumaroles with alteration zone in Garabbayis

Ground temperature measurement at Garabbayis fumaroles

Gas sampling at Garabbayis fumaroles

Fumaroles at the north of survey area (center)

Altered clay at the fumarole point

Altered basalt at the site

Altered rock at the site: calcite vain are common

Existing test well in Garabbayis (Garabbayis-2)

Existing test well in Hanle

Plants at the site

Animals at the site

Outside view of the hotel in Dikhil (nearest accommodation from the site)

Meals at the hotel

Flash flood by torrential rain (on 5th May 2015)

Hanle Plain flooded by torrential rain (on 5th May 2015)

Appendix -3 Existing Well Data

Appendix-3 Existing Well Data

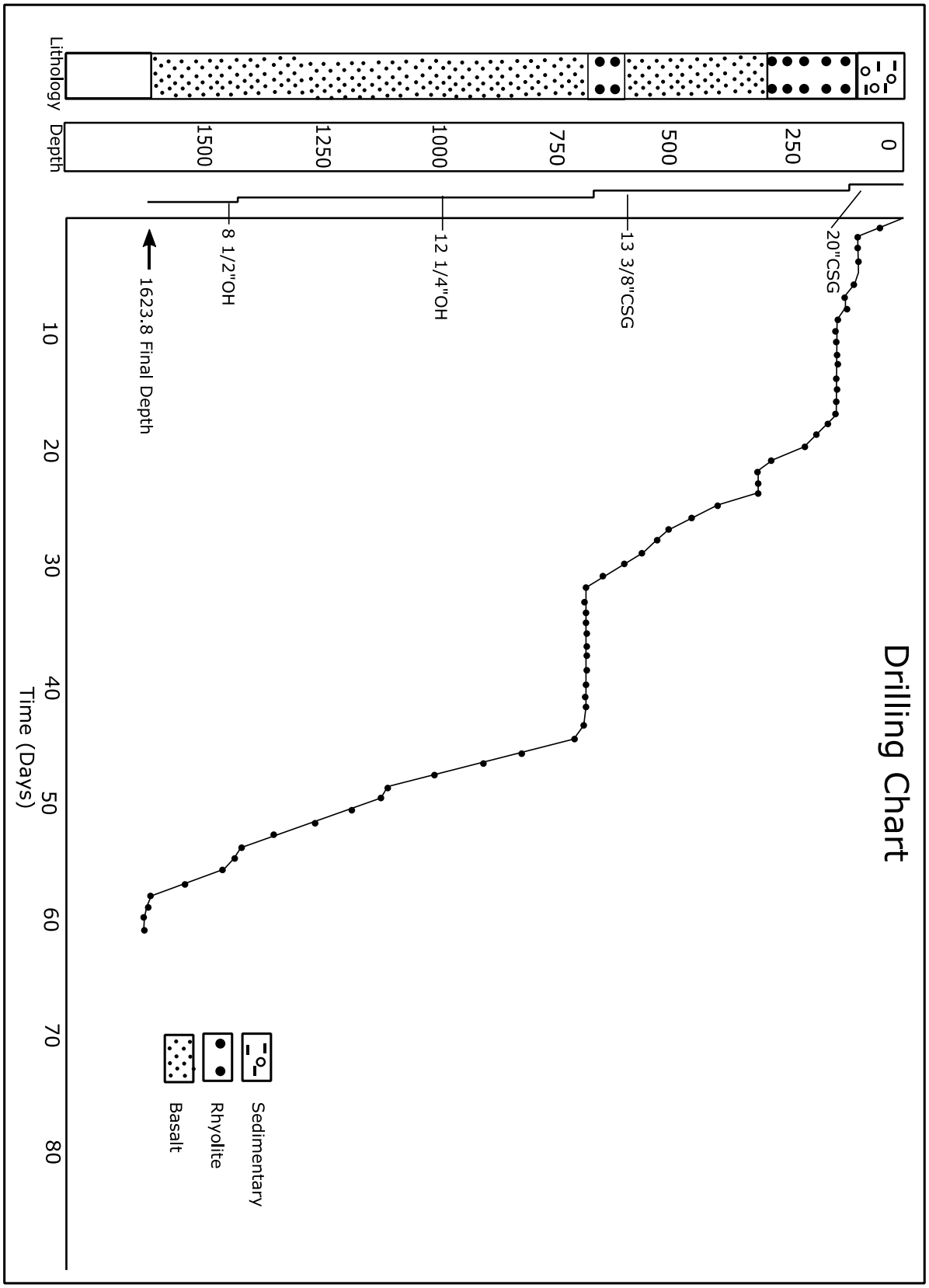

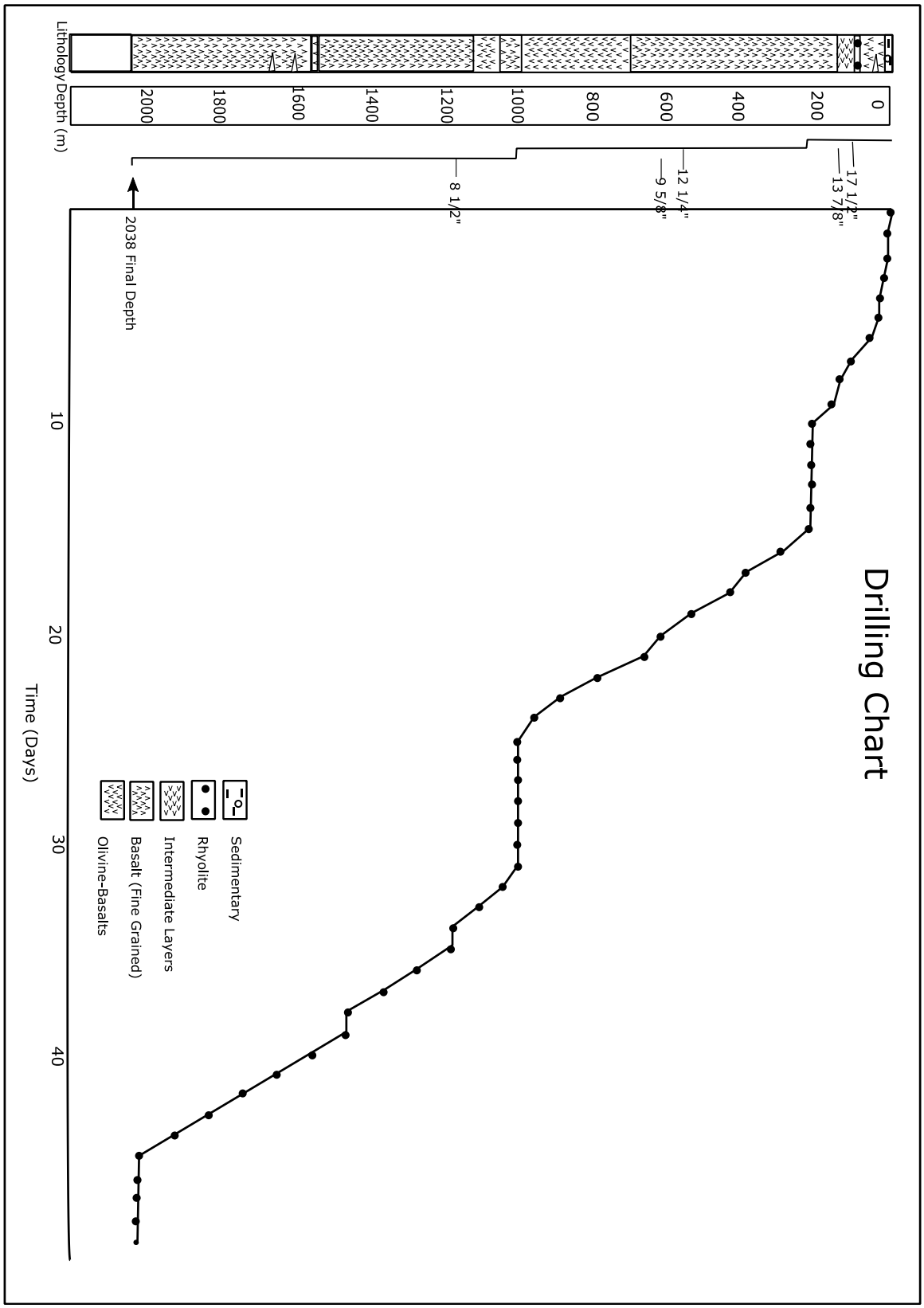

Hanle-2

Aquate r (1987b)

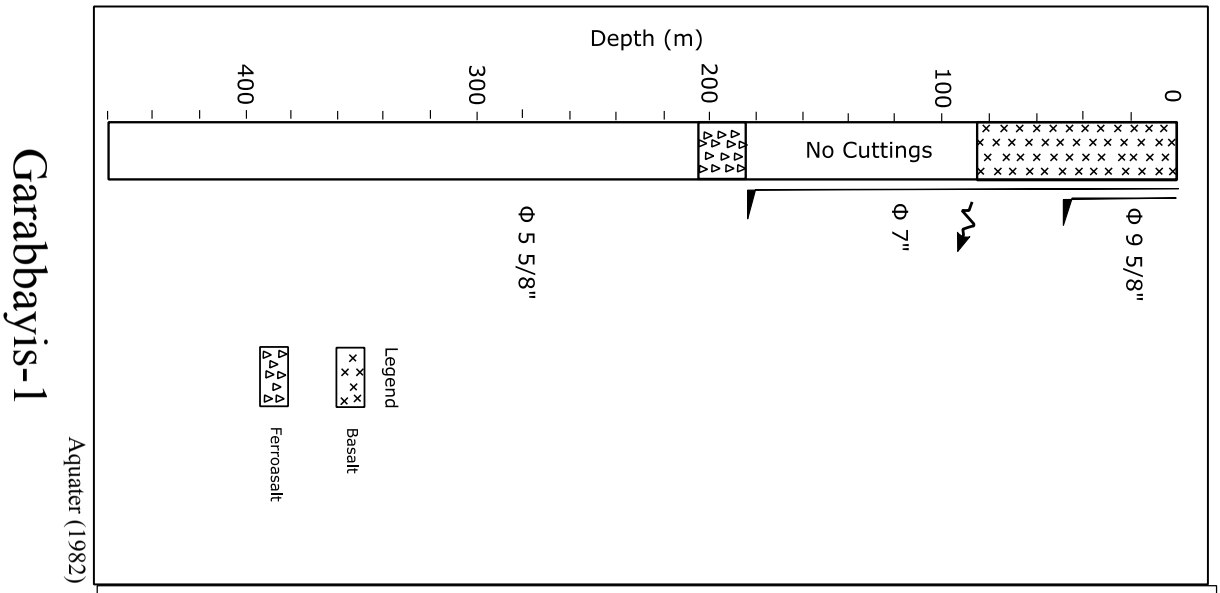
Garabbayis-1
Depth (m)
0
100
200
300
400
No Cuttings
Φ 9 5/8"
Φ 7"
Φ 5 5/8"
Legend
Basalt
Ferroasalt
Aquater (1982)

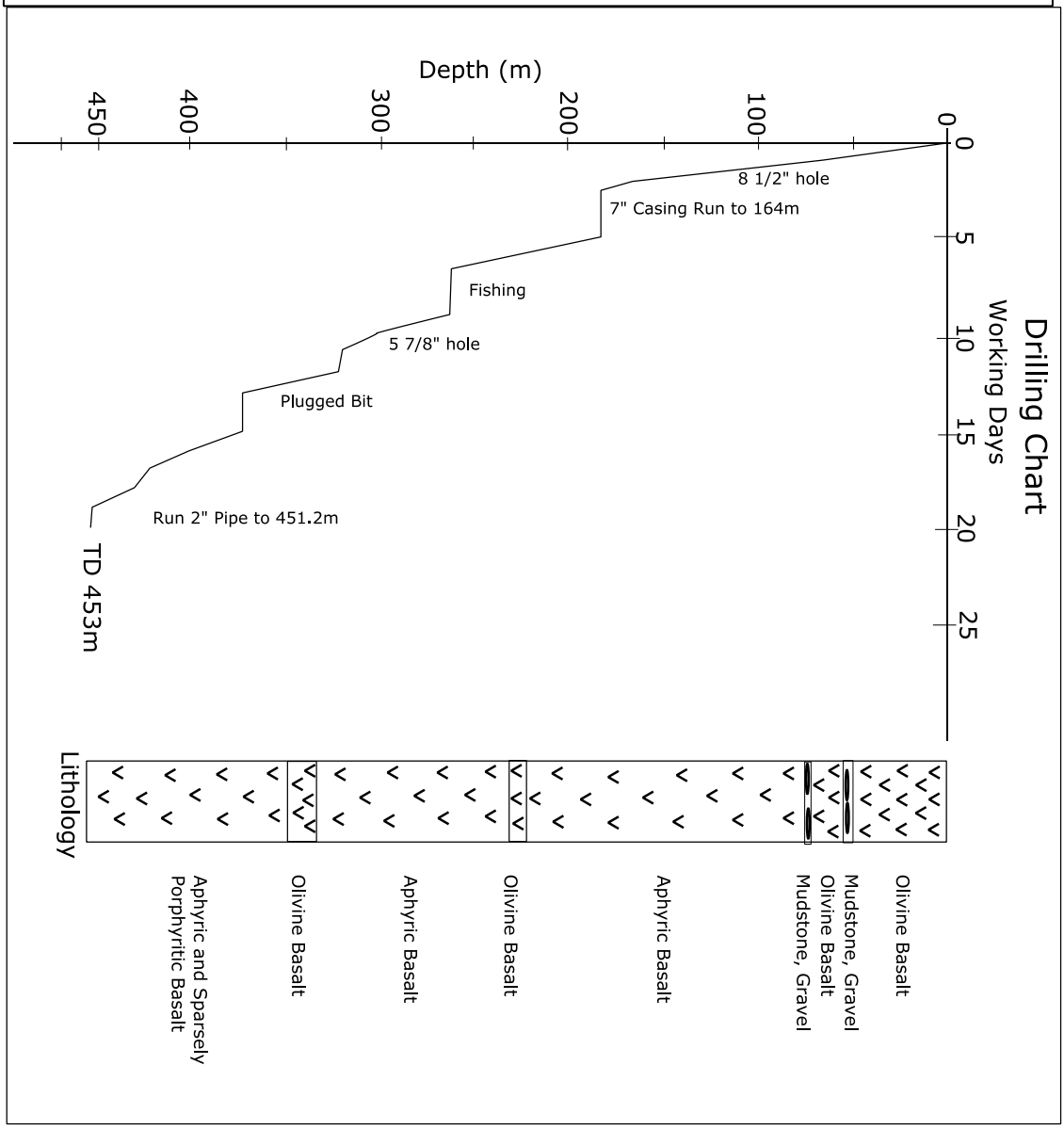
Garabbayis-2
Depth (m)
0
100
200
300
400
450
8 1/2" hole
7" Casing Run to 164m
Fishing
5 7/8" hole
Plugged Bit
Run 2" Pipe to 451.2m
TD 453m
Drilling Chart
Working Days
0
5
10
15
20
25
Lithology
Olivine Basalt
Mudstone, Gravel
Olivine Basalt
Mudstone, Gravel
Aphyric Basalt
Olivine Basalt
Aphyric Basalt
Olivine Basalt
Aphyric and Sparsely Porphyritic Basalt
Geotermica (1985)

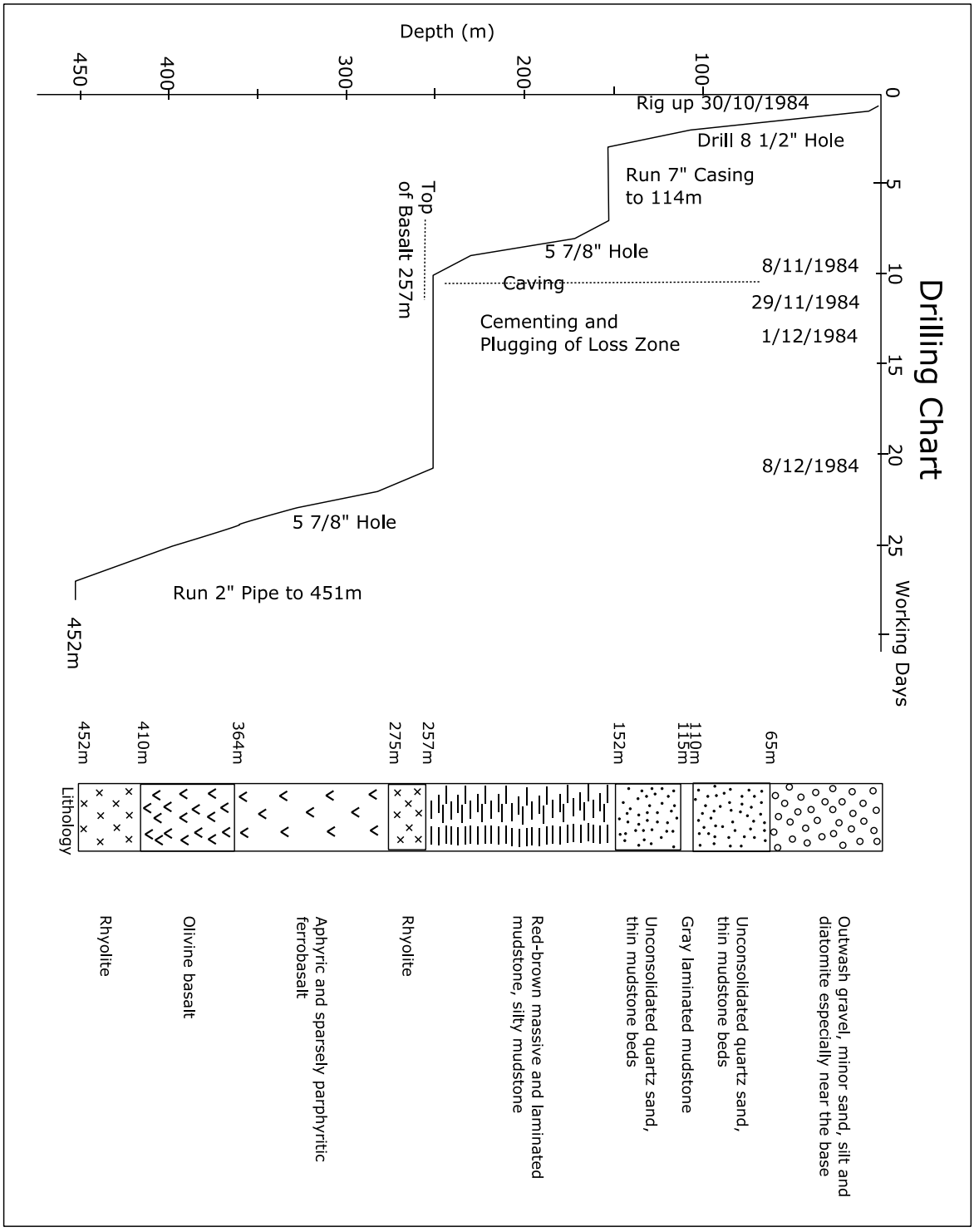

Geotermica (1985)

Appendix -4 MT/TEM Survey

Appendix-4 MT/TEM Survey

4.1 MT Survey

4.1.1 Principle of Method

MT (Magnetotelluric) method observes the earth's magnetic field and telluric current in nature with magnetic and electric sensors to investigate underground structures. MT method can investigate more than 10000 m deep.

The term "MT method" is an abbreviation for magnetotelluric method, derived from the combination of the earth's magnetism and telluric currents. It denotes a survey method using the earth's telluric currents produced in the ground by variations of the earth's magnetic field (See Figure below).The earth's magnetic field changes naturally and is thought to be due to the earth's magnetic oscillation, less than 1 Hz, driven by solar activity and the earth's magnetic pulsation, more than 1Hz, produced by lightning. MT method observes these activities in the frequency range between 0.001 Hz and 1,000 Hz. Observation is commonly carried out overnight when the noise level is low. The remote reference method eliminates the noise at survey points. It uses an observation result at a reference station more than 50km away from the subject site.

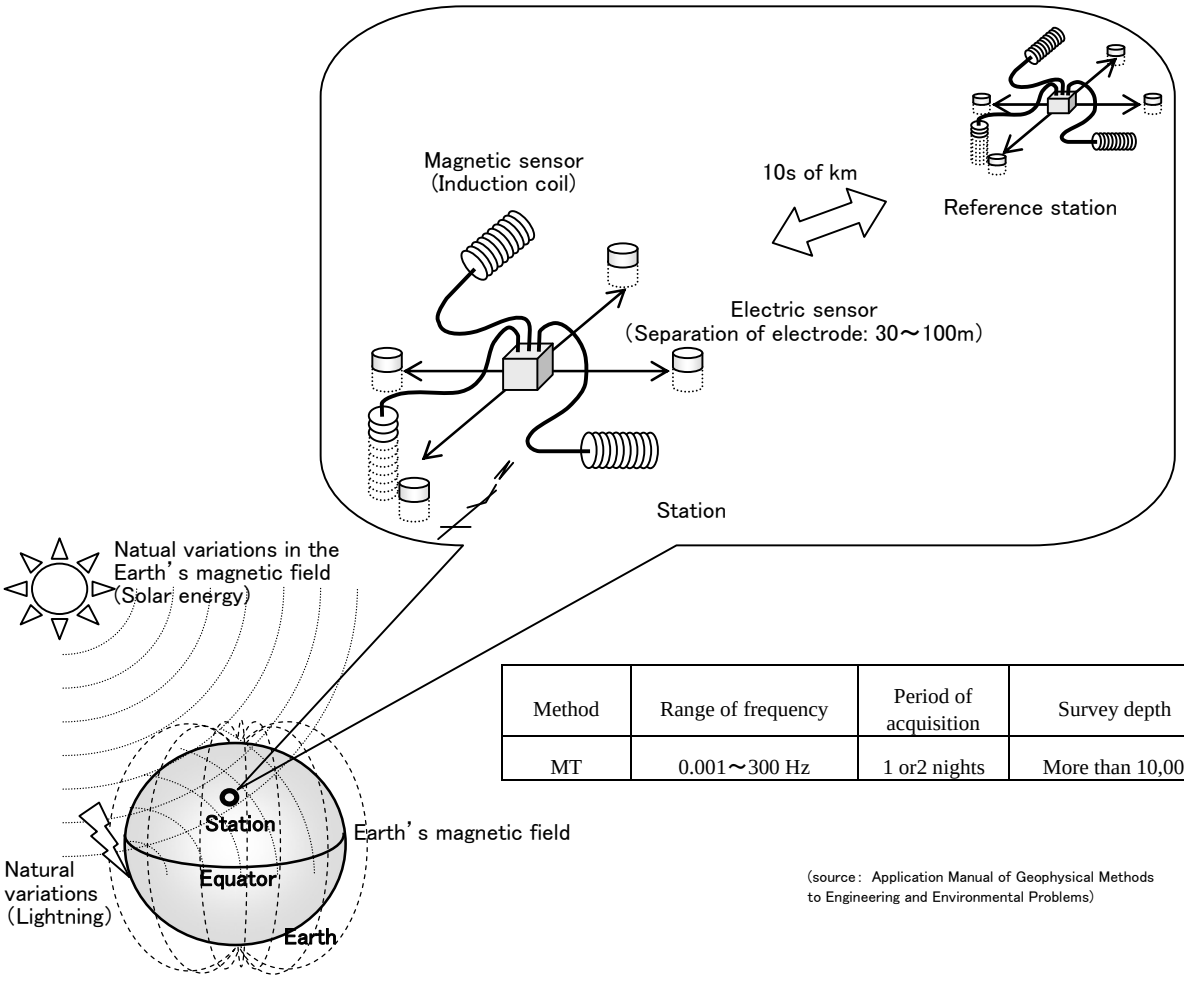

Method	Range of frequency	Period of acquisition	Survey depth
MT	0.001～300 Hz	1 or2 nights	More than 10,000 m

(source: Application Manual of Geophysical Methods to Engineering and Environmental Problems)

Figure : Schematic diagram of principles of MT method

The electromagnetic wave is attenuated gradually while it enters ground surface and penetrates underground. MT method is some of the

The skin depth where the energy intensity decreases to 1/e (about 0.37time) of the intensity at ground surface is regarded as a rule of thumb of the exploration depth for MT method.

The skin depth δ (m) depends on resistivity of ground ρ (ohm-m) and frequency f (Hz) of electromagnetic wave and is estimated as the following equation.

$$\delta = \sqrt{\frac{\rho}{\pi f \mu}} \cong 503\sqrt{\frac{\rho}{f}}$$

Where μ is electric permeability.

This equation shows that the higher the resistivity and the lower the frequency, the deeper the exploration depth into the ground. About MT method in the frequency range of 300 ~ 0.001Hz, the resistivity of 10ohm-m indicates the skin depth of about from 92m to 50km. It is said that the exploration depth of MT method is about 2-1/2 (≒0.707) of the skin depth.

As the variations of the earth's magnetism and telluric currents in low frequencies like the micropulsation affected by solar activity are observed for MT method, the measurement has to be carried out overnight when the culture noise level is low at least for one night. However at MT measurement, the variations of the earth's magnetism and telluric currents are small and it is difficult to distinguish those signals from noises. The remote reference station is set up at the far place from the survey site and where noise is low and the measurement is carried out at the survey station and the remote reference station simultaneously. The variations of observed signals at the survey station which have the correlation with data at the remote reference station are recognized as correct signals and those signals reduce affection of noise to acquired data. This technique is called the remote reference method.

The resistivity is the electrical property obtained from the electromagnetic or electric surveys including MT method. The definition of resistivity is electric resistance per unit of length with electric current flowing through the unit cross section area. This means, the apparent resistivity value is different depending on the directions of the measurements in case of layered underground or fracture rock. In other words, the resistivity shows anisotropy. MT method routinely measures this apparent anisotropy of resistivity differently from electromagnetic surveys except for MT method or electric surveys. For example, in case of the survey for fault, the resistivity in parallel with the strike direction of fault is TE mode and that of the orthogonal direction of the strike is TM mode.

In MT method, generally **Hx** as magnetic field and **Ex** as electric field in NS direction (x axis) and **Hy** and **Ey** in EW direction (y axis) are observed. Bold characters mean complex number. The definition of impedance tensor **Z** is expressed as the next equation with the relationship of magnetic and electric field.

$$\begin{pmatrix} \mathbf{E}_x \\ \mathbf{E}_y \end{pmatrix} = \mathbf{Z}\begin{pmatrix} \mathbf{H}_x \\ \mathbf{H}_y \end{pmatrix} = \begin{pmatrix} \mathbf{Z}_{xx} & \mathbf{Z}_{xy} \\ \mathbf{Z}_{yx} & \mathbf{Z}_{yy} \end{pmatrix}\begin{pmatrix} \mathbf{H}_x \\ \mathbf{H}_y \end{pmatrix}$$

The resistivity is related to the mutually-perpendicular components Zxy and Zyx of impedance tensor. Therefore 2 orthogonal directions of the resistivity are obtained in MT method. If x axis is rotated from NS direction to another, each component value of impedance tensor Z is varied. It means that by using the impedance tensor Z calculated from the observed data at NS and EW directions, the resistivity at arbitrary direction can be estimated.

4.1.2 **Measurement Method**

Next figure shows the schematic drawing for deployment of MT data acquisition system in the project. For data acquisition, MTU-5A system of Phoenix Geophysics (compatible with MT/AMT) was used and 2 components of the electric field and 3 components of the magnetic field were observed as time series. at each station.

The Pb-$PbCl_2$ non-polarized electrodes PE4 of Phoenix Geophysics were used at the measurement of the telluric current and according to the condition of each station, the dipole of 50~100m range was selected. The 2 directions of the dipole were NS and EW direction referring the magnetic north as standard. The electrodes were buried with water and bentonite to reduce contact resistivity in the hole of about 30m depth.

At the measurement of the magnetic field, the induction coils MTC-50/80 of Phoenix Geophysics were used to observe the magnetic field in the direction of NS and EW (magnetic north as standard) and verticality.

The remote reference stations were set up at more than 60 km far from the survey sites. The measurements were conducted simultaneously at the survey station and the remote reference station for more than 14 hours overnight and the survey equipment were moved and set up at next station during daytime. At the beginning of each survey, the calibration was executed to test magnetic sensors and decide coil coefficients.

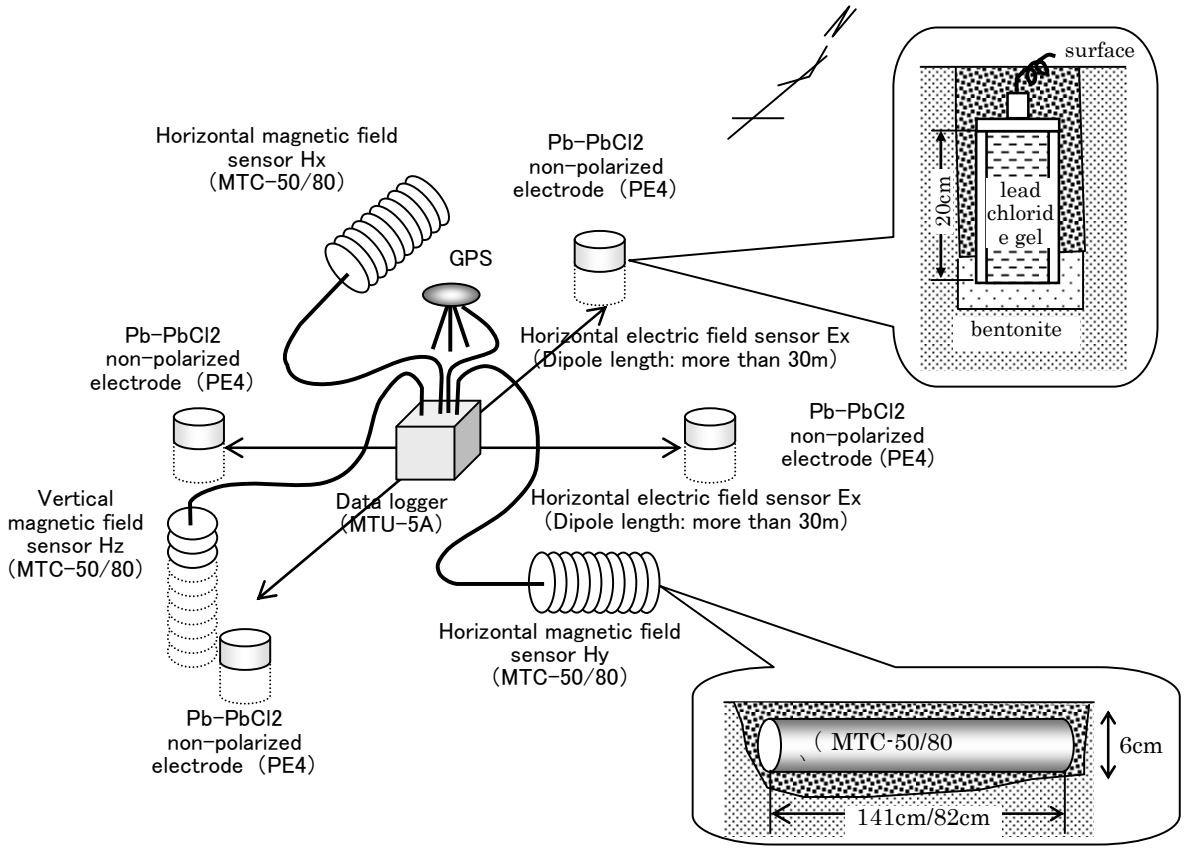

Figure : Schematic drawing for deployment of MT data acquisition system

4.1.3 Data Processing

The time series data including 3 components of magnetic field and 2 components of electric field acquired by data logger were moved to the laptop computer soon in the field after finishing the measurement. each component of the time series data was processed by Fourier transform and each power spectrum at every frequency f (Hz) was obtained. The spectral ratios of horizontal magnetic field Hx(f) and Hy(f), electric field Ex(f) and Ey(f) compose each component of impedance tensor Z(f) at every frequency. The mutually-perpendicular resistivity ρxy(f), ρyx(f) and phase difference $\Delta\phi$xy(f), $\Delta\phi$yx(f) were computed from the impedance tensor Z(f) using the next equation.

$$\rho_{xy}(f) = \frac{1}{2\pi f\mu}\left|\mathbf{Z}_{xy}(f)\right| = \frac{1}{5f}\frac{\left|\mathbf{E}_x(f)\right|}{\left|\mathbf{H}_y(f)\right|}, \quad \Delta\phi_{xv}(f) = \phi\{\mathbf{H}_y(f)\} - \phi\{\mathbf{E}_x(f)\}$$

$$\rho_{yx}(f) = \frac{1}{2\pi f\mu}\left|\mathbf{Z}_{yx}(f)\right| = \frac{1}{5f}\frac{\left|\mathbf{E}_y(f)\right|}{\left|\mathbf{H}_x(f)\right|}, \quad \Delta\phi_{xv}(f) = \phi\{\mathbf{H}_y(f)\} - \phi\{\mathbf{E}_x(f)\}$$

Where,

f: frequency (Hz), π: the ratio of the circumference of a circle to its diameter, μ: magnetic permeability

$|\mathbf{E}_x(f)|$、$|\mathbf{E}_y(f)|$: intensity of electric field (V/m), $|\mathbf{H}_x(f)|$, $|\mathbf{H}_y(f)|$: intensity of magnetic field (nT)

$\phi\{\mathbf{E}_x(f)\}$, $\phi\{\mathbf{E}_y(f)\}$: phase of electric field (degree), $\phi\{\mathbf{H}_x(f)\}$, $\phi\{\mathbf{H}_y(f)\}$: phase of magnetic field (degree)

Calculated resistivity ρxy(f) and ρyx(f) mean exact resistivity in case that the ground resistivity is equal. Actually, as they mean approximate resistivity because of the unequal ground resistivity, it is called "apparent resistivity" in MT method. Phase difference is called "phase" ϕxy(f), ϕyx(f). An example of apparent resistivity and phase curve is shown in Figure below.

In the project, the observed time series data were divided to 20 segments and each apparent resistivity and phase is calculated at every segment. 20 processed values were obtained at every frequency and statistically mean and variance are calculated and variance is expressed as error bar on apparent resistivity curve or phase curve. Generally, it is desirable and means high quality to have low scatter, moderate curvature and well-joined frequency-band curve segments. Data processing by using only the observation data at survey station is called local processing. In the project, after downloading data to the laptop computer, the local processing was done and data quality of the observed data was estimated with the apparent resistivity and phase curve.

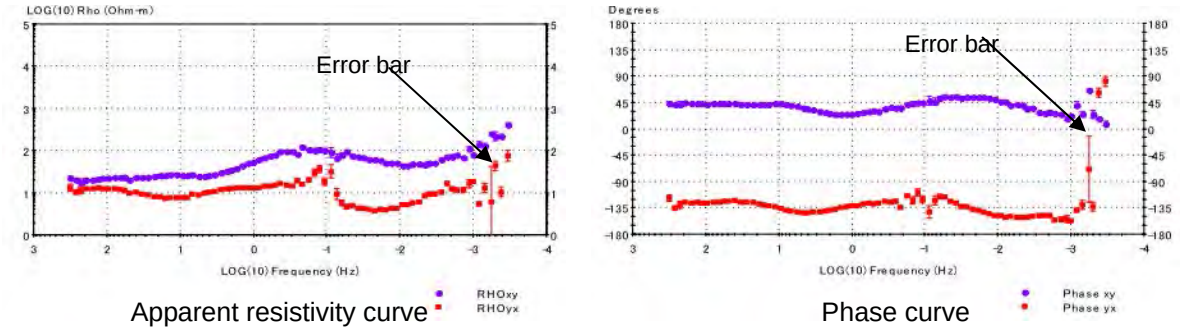

Figure : An example of an apparent resistivity and phase curve

About data processing of this survey, at 80 frequencies in the range between 320 Hz ~ 0.00034 Hz of MT data, each impedance tensor Z(f) was computed.

After the field survey finishing, by using the acquired data at remote reference station, the remote reference processing technique was applied to the acquired data at survey stations to remove local noises. A concept of remote reference processing is given in the next figure. Both the observed data and the remote reference data have artificial electromagnetic noises generated by power lines, residences, and traffic of vehicles etc. in circles of Figure. If the distance between the survey site and the remote reference station is fully far, the correlation of the signal is good and at the same time, noise shows no correlation. Therefore after cross-correlation data processing, the processed data without noise are created.

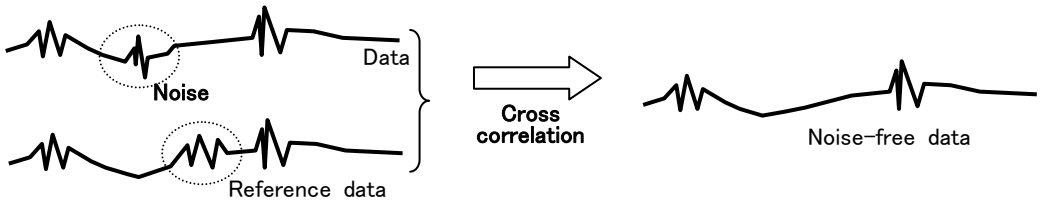

Figure : A concept of remote reference processing

SSMT2000 software of Phoenix Geophysics was used for a series of remote reference data processing technique. The processed data were edited by selecting the segment with high S/N at every frequency so that the apparent resistivity and phase curves have small error bar and smooth curvature. For edit, MT-editor software of Phoenix Geophysics was used.

4.1.4 Data Analysis

As mentioned above, the apparent resistivity ρxy(f) and ρyx(f) computed through data processing just indicate the mean value of resistivity to the exploration depth (about 0.707times skin depth). 2D inversion analysis was executed using apparent resistivity and phase curves to infer the resistivity structure.

For data analysis, considering the comprehensive strike directions of the survey site, profiles were set up and y axis was put in the direction of the profile and x axis was put in the perpendicular direction of the profile.

Impedance tensor was rotated and the apparent resistivity from the combination of electric field of x direction and magnetic field of y direction as TE mode (parallel to structure) and the apparent resistivity from the combination of electric field of y direction and magnetic field of x direction as TM mode (perpendicular to structure) are computed respectively and used for 2D inversion as input data.

In 2D inversion , under the assumption that the resistivity structure doesn't change and continue infinitely in the direction perpendicular to profile, 2D resistivity model is computed automatically so that the response of 2D resistivity model fits to the observed impedance. The resistivity value of each cell in the resistivity model is calculated from all apparent resistivities of the profile by non-linear least squares method. As apparent resistivity of adjacent survey station and adjacent resistivity cell are considered, a relatively continuous model is obtain as reasonable analysis result.

In the project, 2D resistivity inversion analysis was executed using WinGLink of Schlumberger Inc. which has an function of 2D inversion. The cross section of profile is composed by the elements of finite element method for model calculation and resistivity cells combined by elements. The size of the element and the resistivity cell are made enough fine at shallow zone and larger to the direction of marginal and deep zone.

And next, the homogeneous model of 100 ohm-m resistivity is used as initial model and the response of resistivity model by finite element method was computed at each survey station. Comparing the calculated apparent resistivity with the observed apparent resistivity, the iteration of correcting resistivity was

continued until RMS (abbreviation of Root Mean Square) error becomes less than the threshold.

4.2 TEM Survey

4.2.1 Principle of Method

TEM method is an abbreviation for transient electromagnetic method. It means a method that observes the transients of magnetic field after turning off an input artificial magnetic field (See Figure below).

An artificial magnetic field is transmitted in a vertical direction when an electric current flows in an electric square loop on the ground (transmission loop). The loop may be rectangle or circle. When the electric current is turned off, a secondary electric current starts in the ground in a circle to maintain the input magnetic field. This current gradually spreads under the ground further. This current is called the eddy current, or often called "smoke ring" comparing to the smoke loop from cigar. The input artificial magnetic field decays in time and its rate is less where the resistivity is low. The resistivity of the subsurface is estimated by measuring the decay of the artificial magnetic field by an induction (receiver) coil. The decay immediately after stopping the current signal (early time response) indicates resistivity at shallow ground and the late time response resistivity at deeper parts.

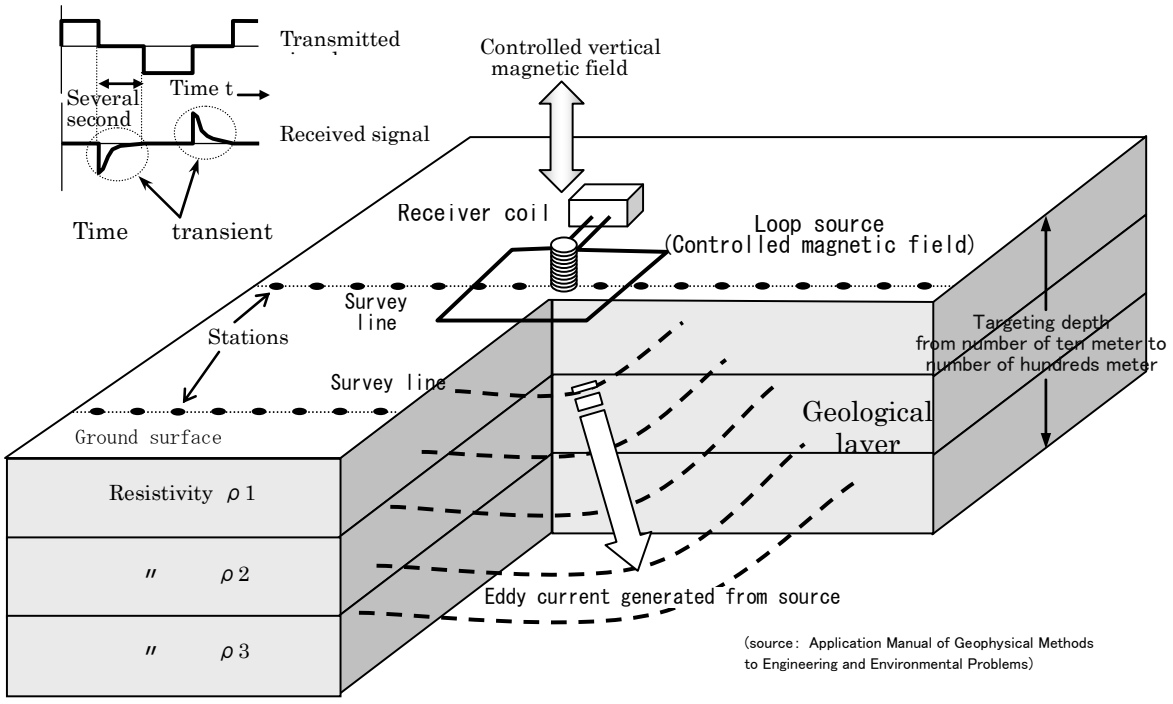

Figure : Schematic diagram of principles of TEM method

Especially, TEM method is useful to the structure which shows low resistivity (high conductance) due to groundwater, argillation, weathered deep layer, alteration etc.

The diffusion depth δ (m) is regarded as a rule of thumb of the exploration depth for TEM method and it is estimated as the following equation.

$$\delta = \sqrt{\frac{2t\rho}{\mu}}$$

Where, ρ: ground resistivity (ohm-m), t: time after turning off the primary field (sec), μ: magnetic permeability

This equation shows that the higher the resistivity and the longer the time, the deeper the exploration depth into the ground.

It is difficult to investigate the structure under the distribution of low resistivity with electric methods at the survey site where low resistivity distributes such as argillation or alteration at the shallower zone. But TEM method is available to investigate deeper zone. Especially, in the survey site where argillation or saline groundwater exists at the surface layer TEM method is suitable.

4.2.2 Measurement Method

In the project, TEM method is used for static correction of MT data. As about 100 m is needed as exploration depth, 100 m square loop was set up on the ground and the current was passed by the portable transmitter to induce magnetic field. After turning off the current, the transient response of magnetic field was measured by the induction coil in the center of the loop for a few times in central loop system. Figure 3.2.6 shows the survey schematic drawing for deployment of TEM data acquisition system in the project. V8 system of Phoenix Geophysics was used and the transient response of vertical magnetic field was measured at each station. The transmitter current is about 3.5A, the number of time windows is 20, the number of stacks is more than 10 times and 2 kinds of the repeat rate 25 Hz, and 2.5 Hz were mainly used.

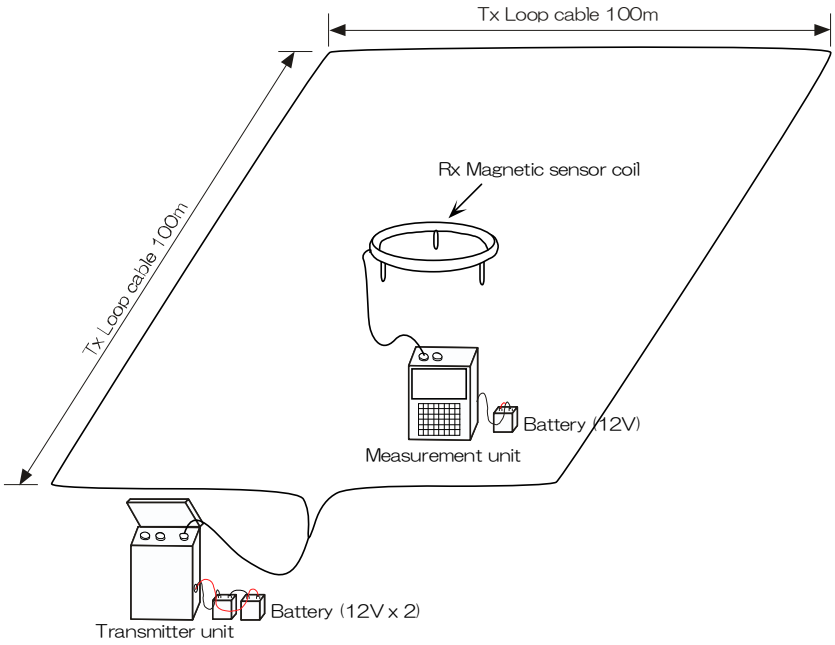

Figure : Schematic drawing for deployment of TEM data acquisition system

4.2.3 **Data Processing and Analysis**

The 1D inversion analysis was carried out from the acquired TEM data. The analysis software is WinGLink of Schlumberger Inc. At each survey station, 5 or 6 layers structure was assumed and the values of resistivity and layer's thickness of the 1D layered model was obtained by 1D inversion analysis so that the transient response of the 1D layered model fitted the observed transient response. An example of the acquired TEM data and the result of 1D layered inversion analysis are shown in the following figure.

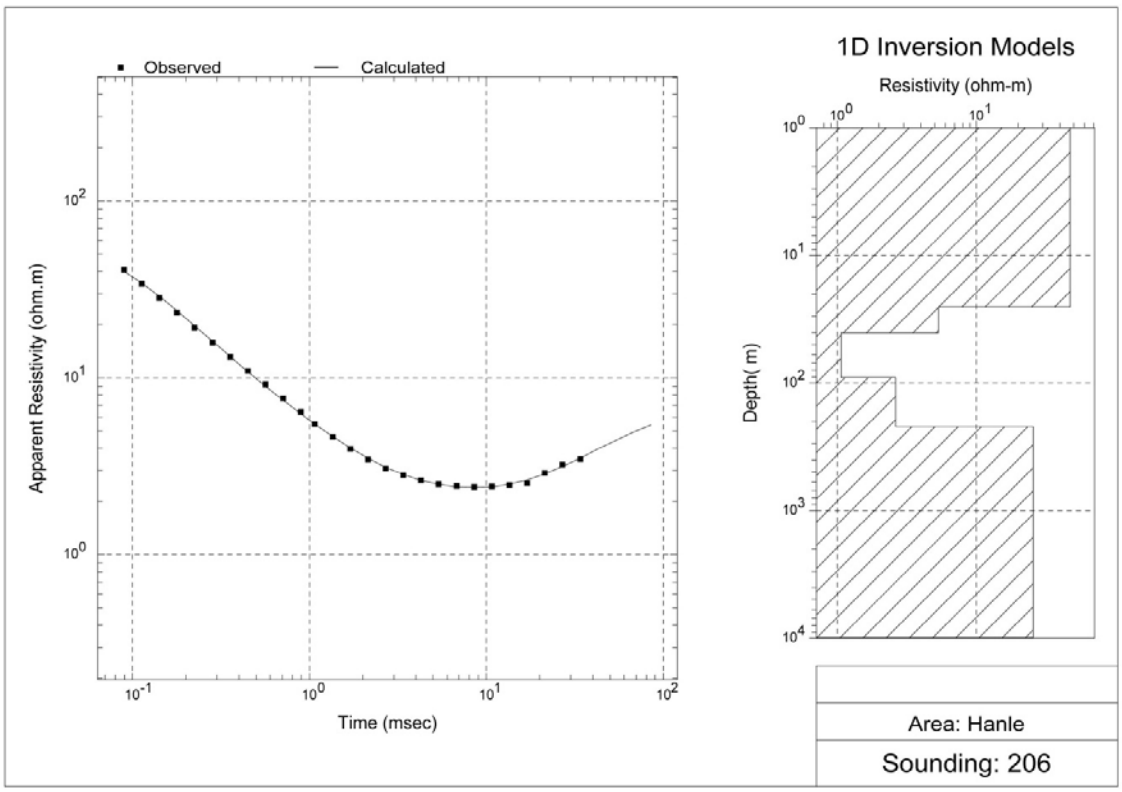

Figure : An example of TEM data analysis

4.2.4 **Static Correction of MT data**

An important feature in the data processes with MT method is static shift. The apparent resistivity curve in the following figure contains a static shift caused by a local resistivity anomaly in the shallow ground near the survey station. Before starting the analysis, it is necessary to move the apparent resistivity curve back to its normal position, where it would be without the anomaly. A qualitative process is used for this purpose, incorporating shallow resistivity information by resistivity or other electromagnetic methods like TEM, or the difference in a pair of apparent resistivity of higher frequency band.

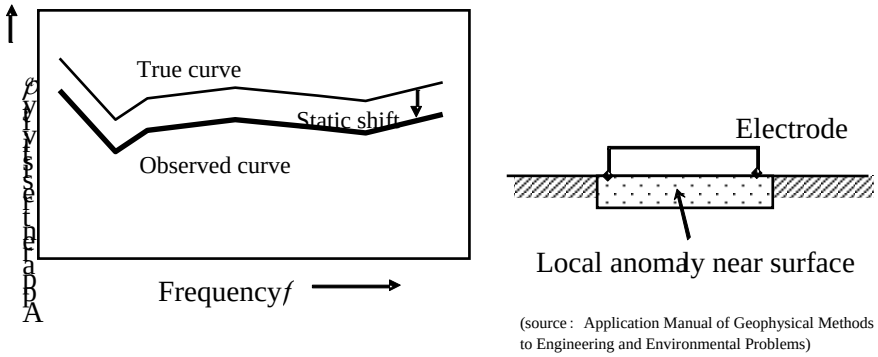

(source : Application Manual of Geophysical Methods to Engineering and Environmental Problems)

Figure : Static-shift due to a near-surface anomaly

Locations of coordinate system of MT stations

Station	Coordinate (WGS84)		Elevation (m)
	Latitude	Longitude	
HNL-101	11°22'42.8"	42°10'36.8"	301
HNL-102	11°23'2.3"	42°10'59.5"	349
HNL-103	11°23'17.9"	42°11'30.6"	356
HNL-104	11°23'40.0"	42°11'55.1"	379
HNL-105	11°23'58.6"	42°12'22.9"	378
HNL-106	11°24'17.0"	42°12'50.0"	393
HNL-201	11°23'16.8"	42°10'7.9"	243
HNL-202	11°23'42.1"	42°10'35.6"	346
HNL-203	11°23'54.0"	42°11'5.4"	364
HNL-204	11°24'12.4"	42°11'32.7"	394
HNL-205	11°24'33.0"	42°11'59.0"	413
HNL-206	11°24'48.1"	42°12'25.6"	413
HNL-301	11°23'53.4"	42°9'49.2"	240
HNL-302	11°24'9.4"	42°10'13.4"	250
HNL-303	11°24'27.3"	42°10'45.7"	298
HNL-304	11°24'47.0"	42°11'8.6"	400
HNL-305	11°25'6.0"	42°11'34.4"	439
HNL-306	11°25'22.4"	42°12'2.7"	431
HNL-401	11°24'26.2"	42°9'20.8"	230
HNL-402	11°24'44.7"	42°9'52.0"	247
HNL-403	11°25'0.1"	42°10'13.6"	267
HNL-404	11°25'19.5"	42°10'45.0"	408
HNL-405	11°25'38.3"	42°11'12.0"	451
HNL-406	11°25'53.8"	42°11'38.0"	454
HNL-501	11°24'57.8"	42°8'55.3"	224
HNL-502	11°25'16.7"	42°9'25.4"	228
HNL-503	11°25'32.5"	42°9'53.4"	272
HNL-504	11°25'47.6"	42°10'18.8"	315
HNL-505	11°26'10.8"	42°10'49.1"	458
HNL-506	11°26'29.4"	42°11'16.2"	476
HNL-900 (MT-Ref: Dikhil)	11°8'12.2"	42°19'8.57"	391

Offset values for static correction

Station	Static Shift (TE)	Static Shift (TM)	Station	Static Shift (TE)	Static Shift (TM)
HNL-101	1.000	1.000	HNL-304	1.079	1.382
HNL-102	1.085	1.464	HNL-305	1.000	1.130
HNL-103	0.914	1.253	HNL-306	1.126	1.000
HNL-104	0.779	1.299	HNL-401	1.000	1.000
HNL-105	1.247	1.000	HNL-402	1.146	1.132
HNL-106	1.211	1.348	HNL-403	1.000	0.230
HNL-201	1.196	0.880	HNL-404	1.162	1.301
HNL-202	1.378	0.928	HNL-405	1.000	1.209
HNL-203	0.918	1.000	HNL-406	1.185	1.000
HNL-204	1.000	1.000	HNL-501	1.044	1.869
HNL-205	1.123	1.072	HNL-502	1.454	1.000
HNL-206	1.117	1.000	HNL-503	1.190	1.785
HNL-301	1.000	1.060	HNL-504	0.437	0.790
HNL-302	1.099	1.163	HNL-505	1.000	1.000
HNL-303	1.000	0.316	HNL-506	1.344	0.759

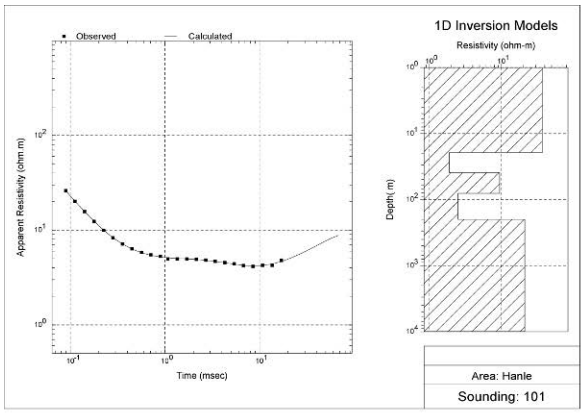

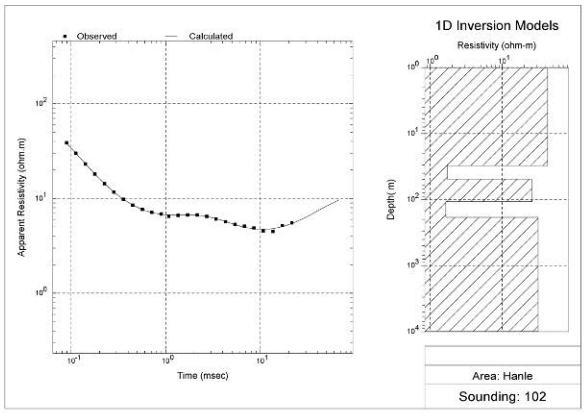

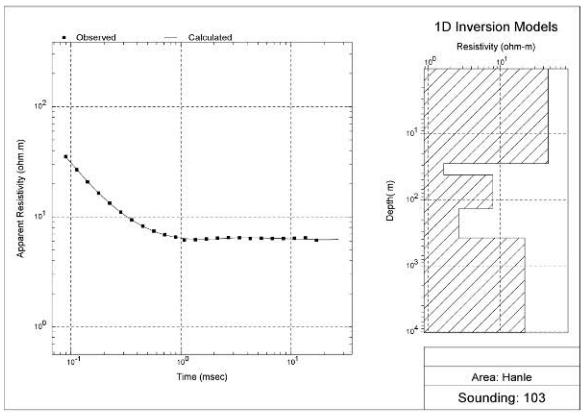

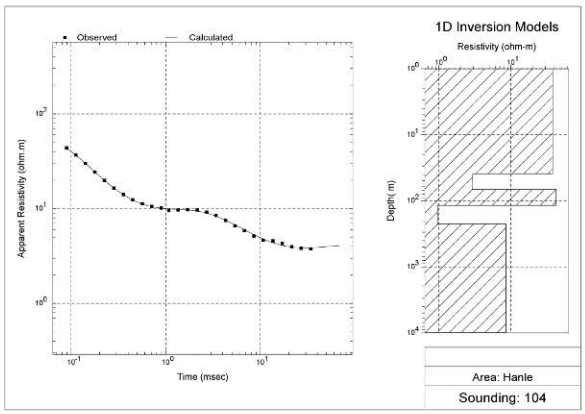

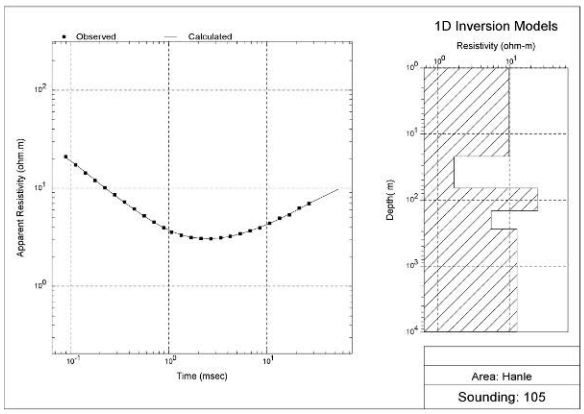

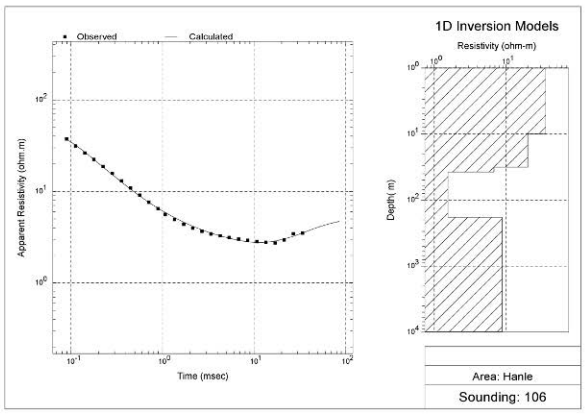

TEM survey results of 1D inversion analysis (HNL100)

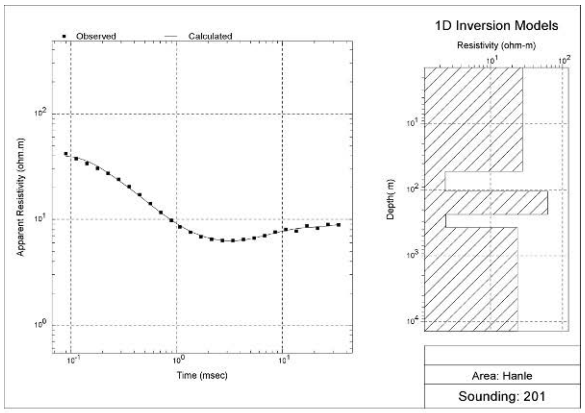

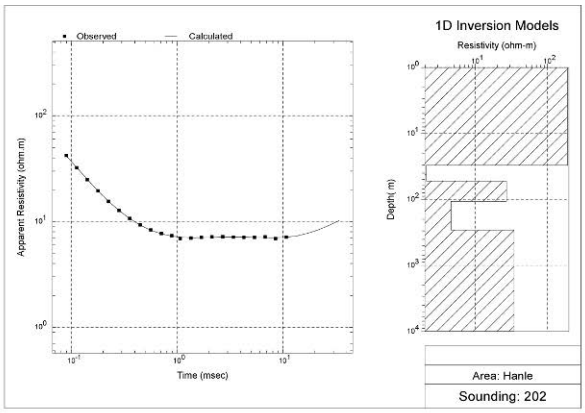

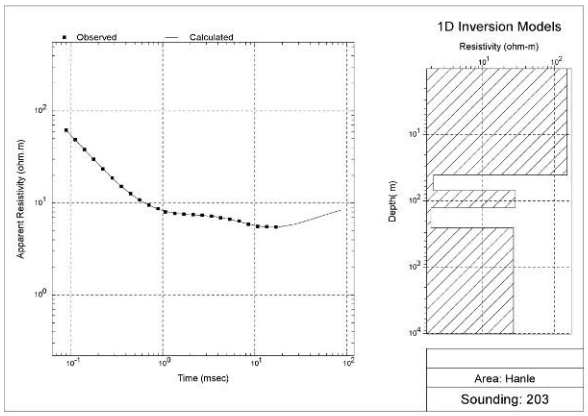

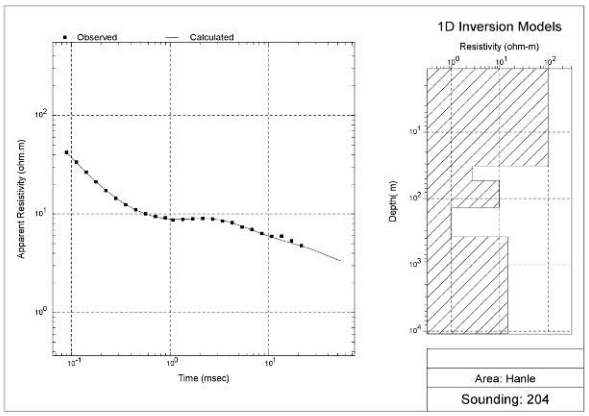

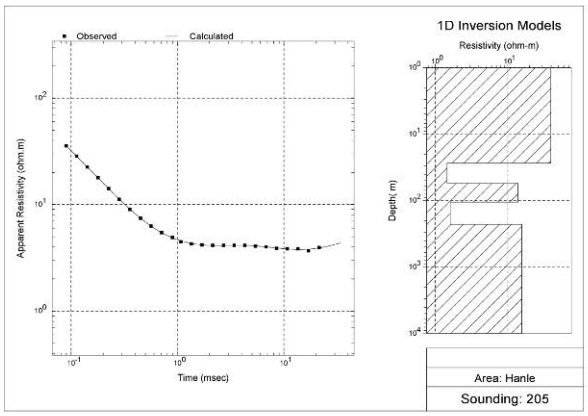

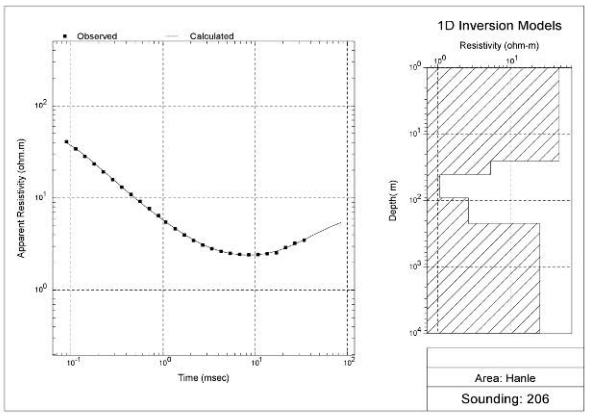

TEM survey results of 1D inversion analysis (HNL200)

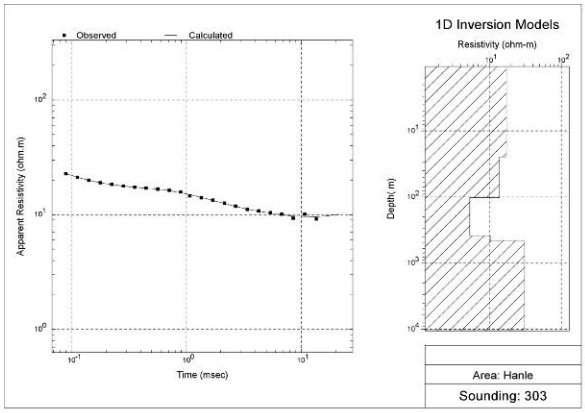

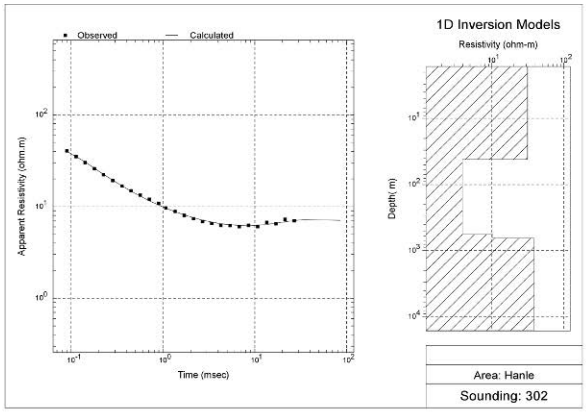

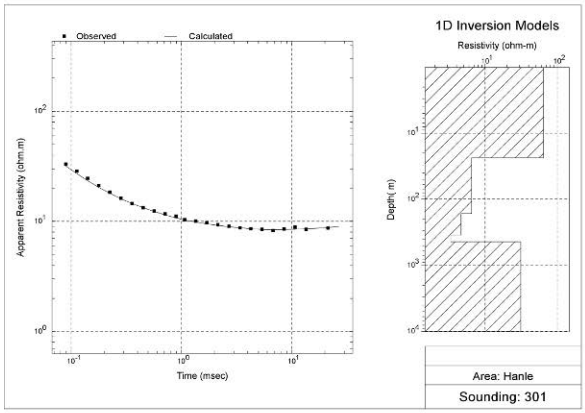

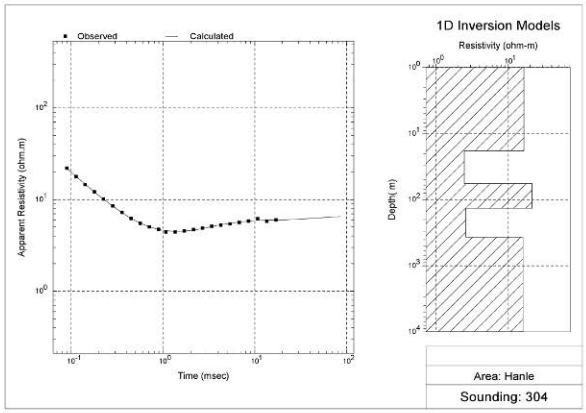

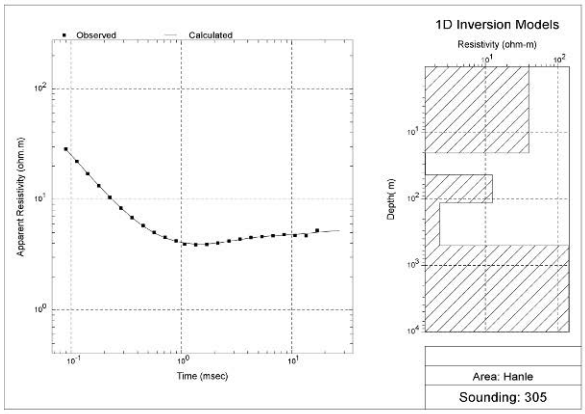

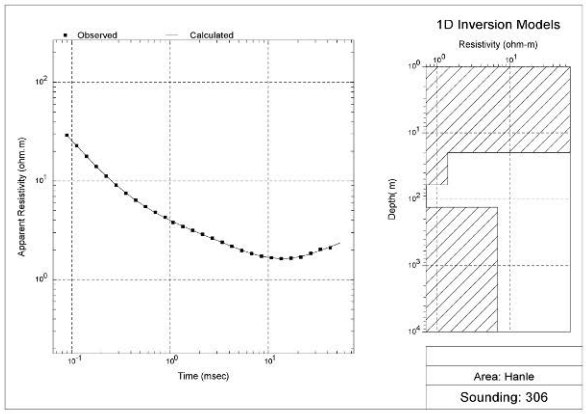

TEM survey results of 1D inversion analysis (HNL300)

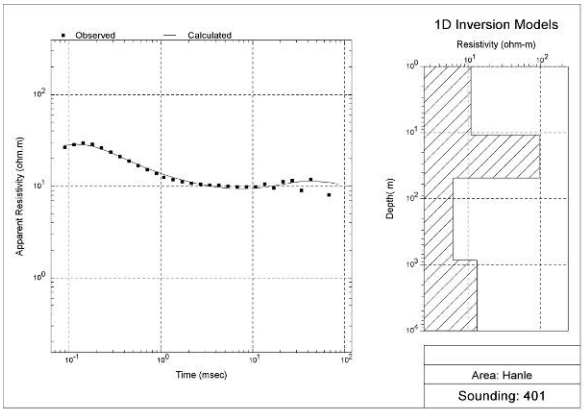

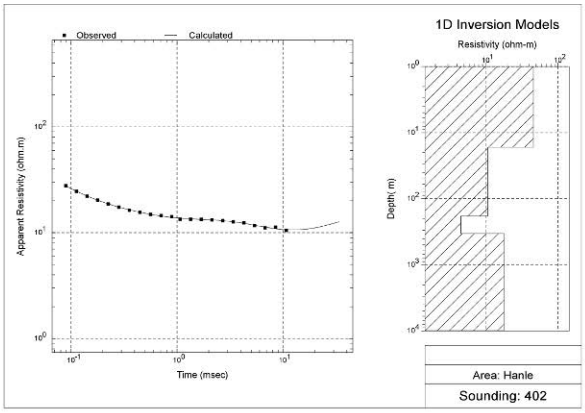

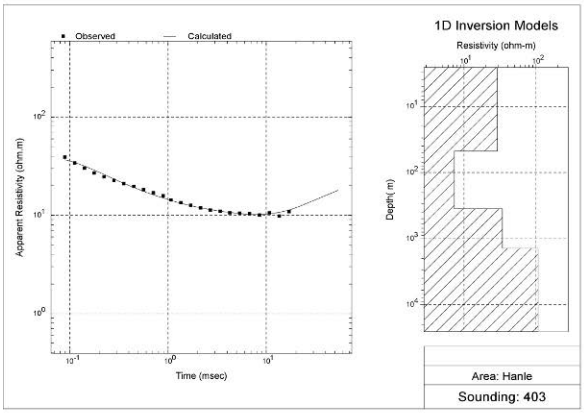

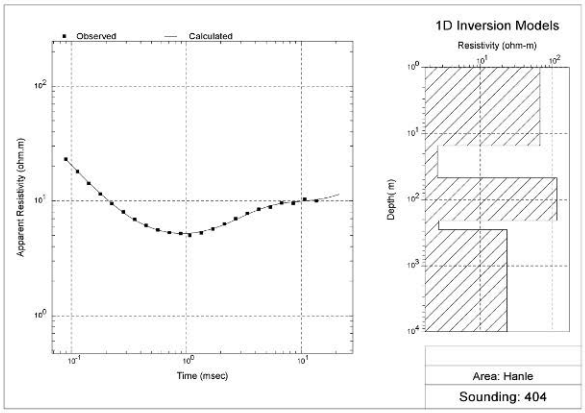

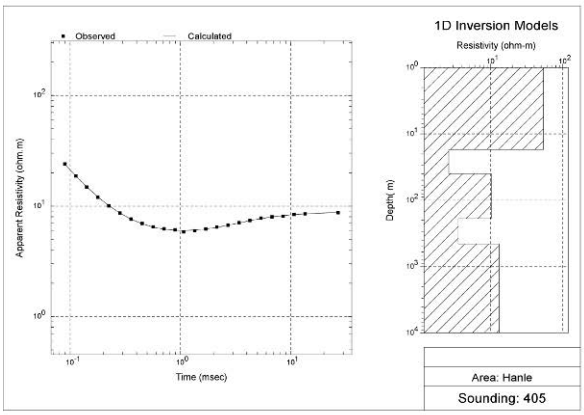

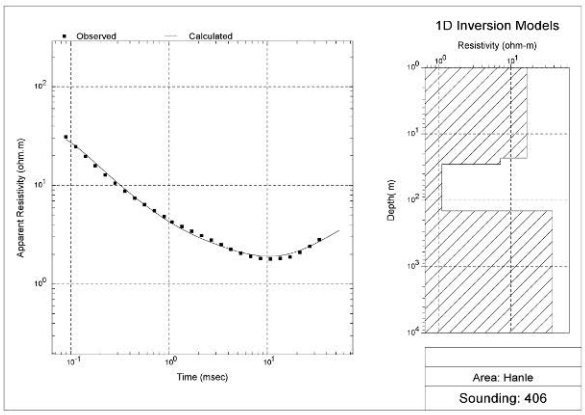

TEM survey results of 1D inversion analysis (HNL400)

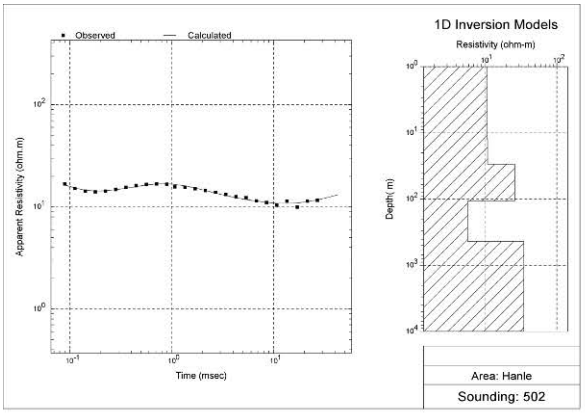

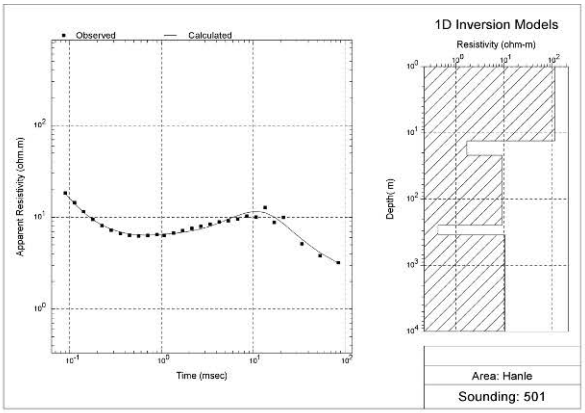

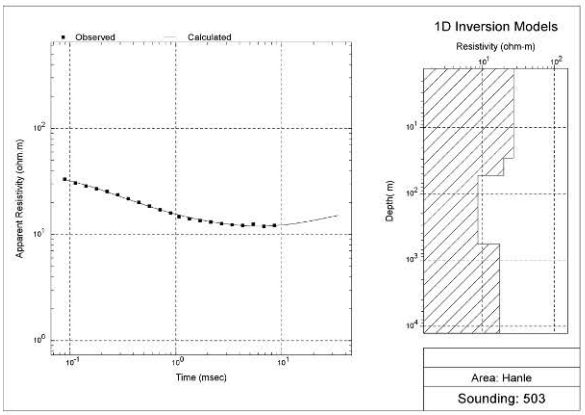

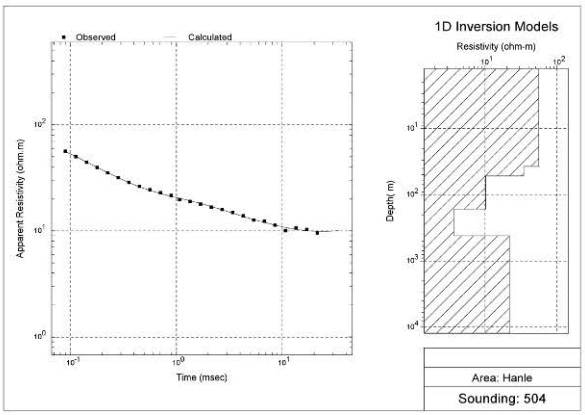

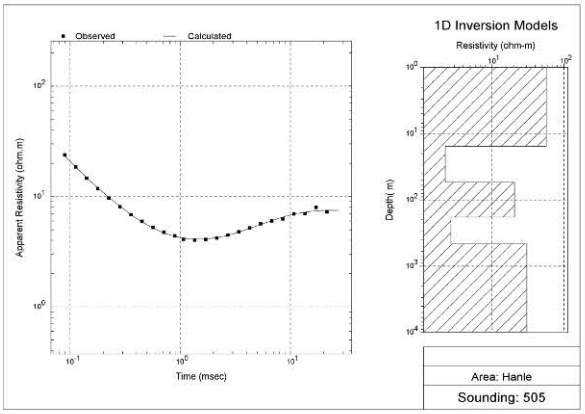

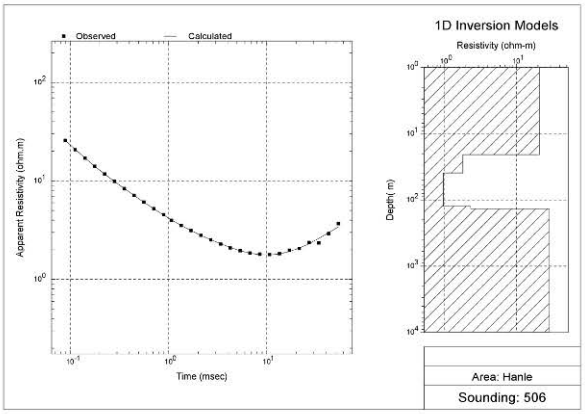

TEM survey results of 1D inversion analysis (HNL500)

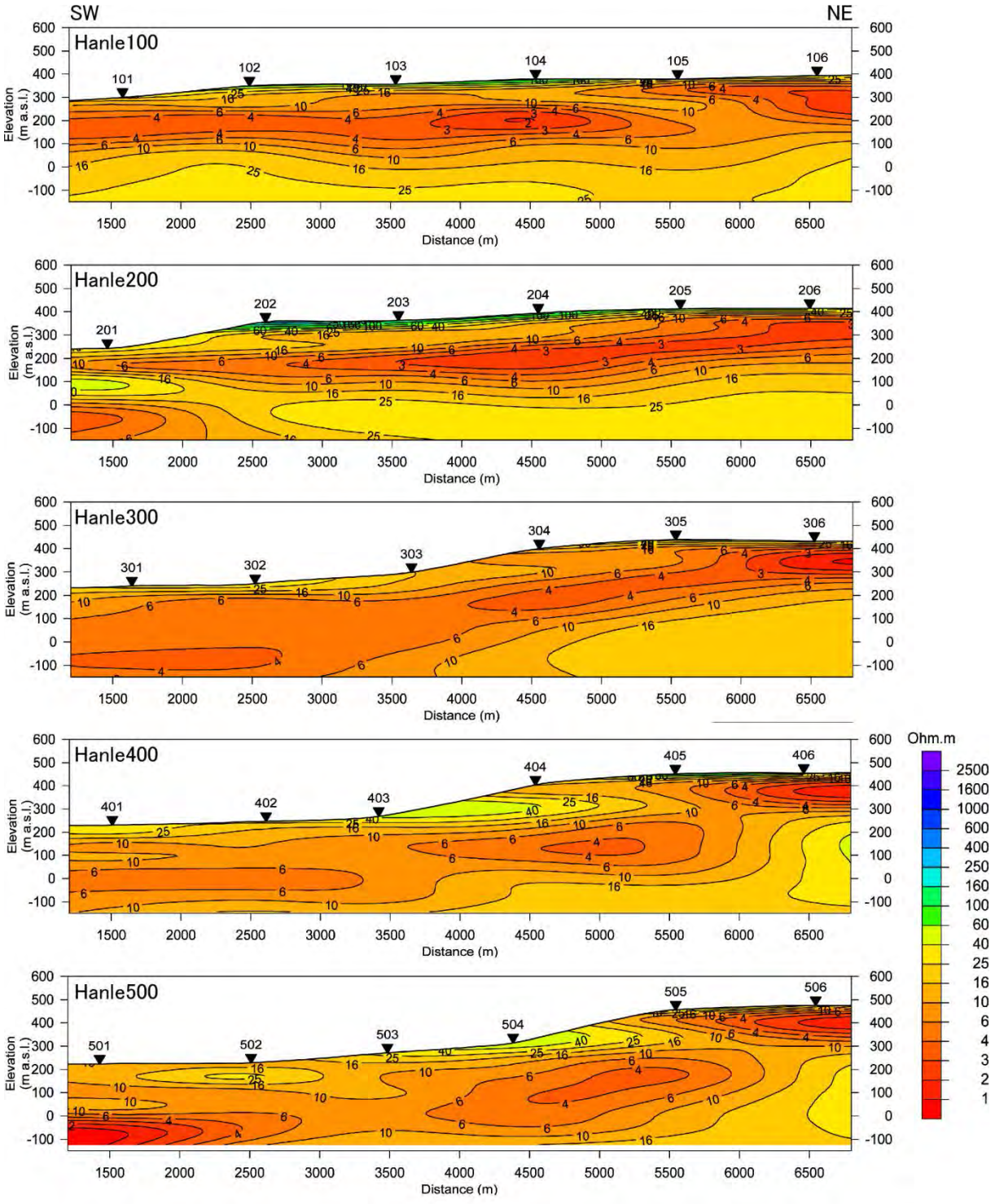

The resistivity cross sections of the very shallow zone from the results of TEM 1D inversion analysis

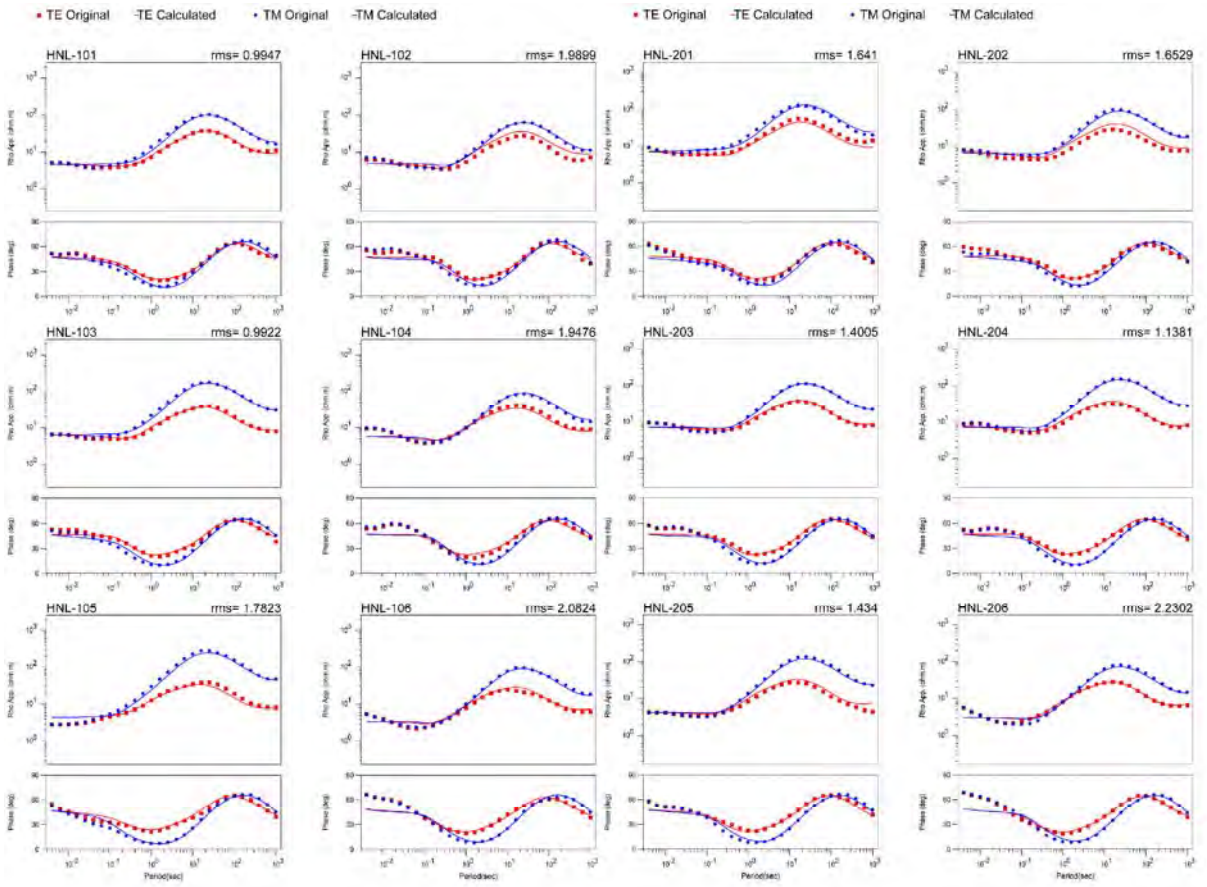

Apparent Resistivity and Phase Difference (HNL100, HNL200)

(Dots: Observed data, Lines: Calculated response)

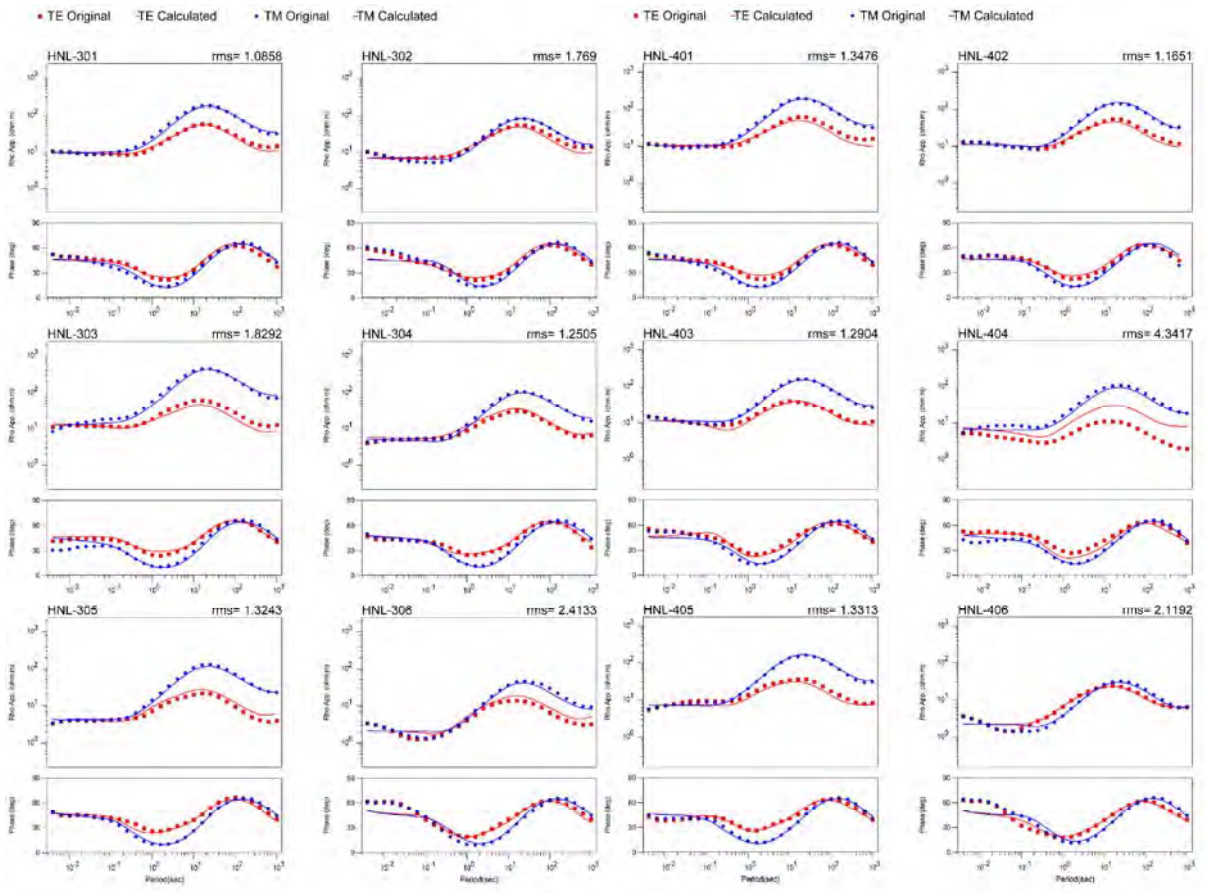

Apparent Resistivity and Phase Difference (HNL300, HNL400)
(Dots: Observed data, Lines: Calculated response)

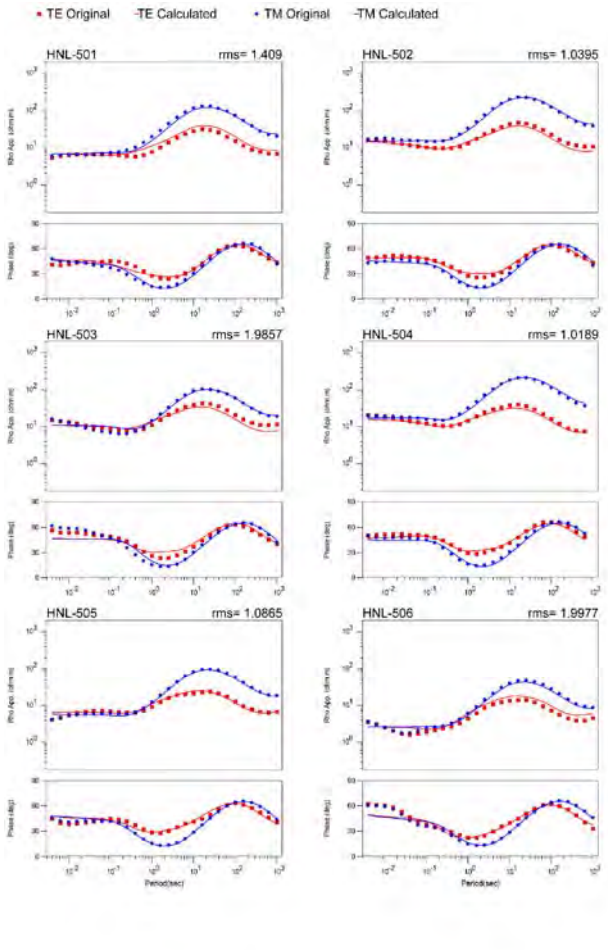

Apparent Resistivity and Phase Difference (HNL500)
(Dots: Observed data, Lines: Calculated response)

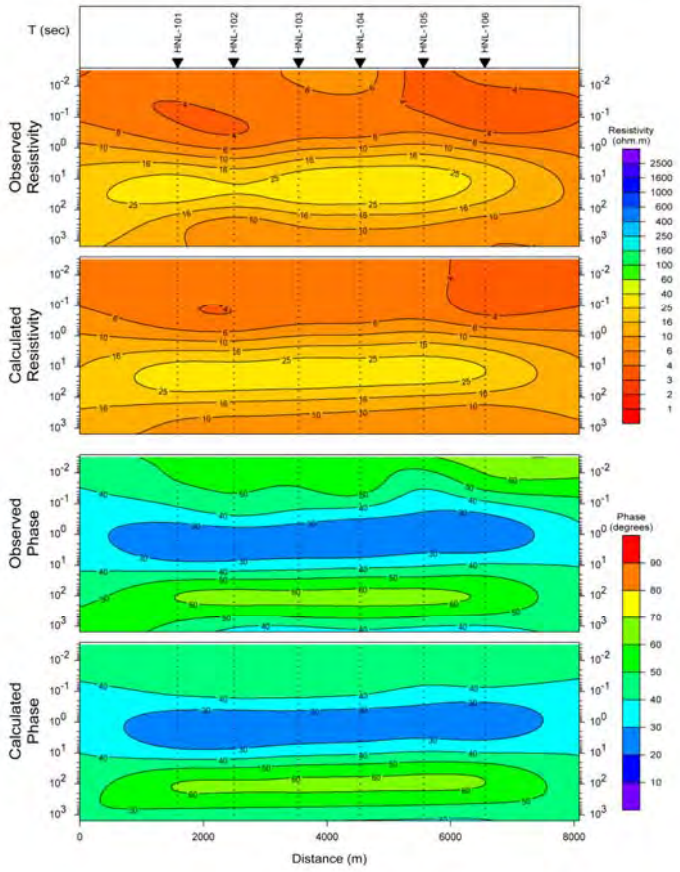

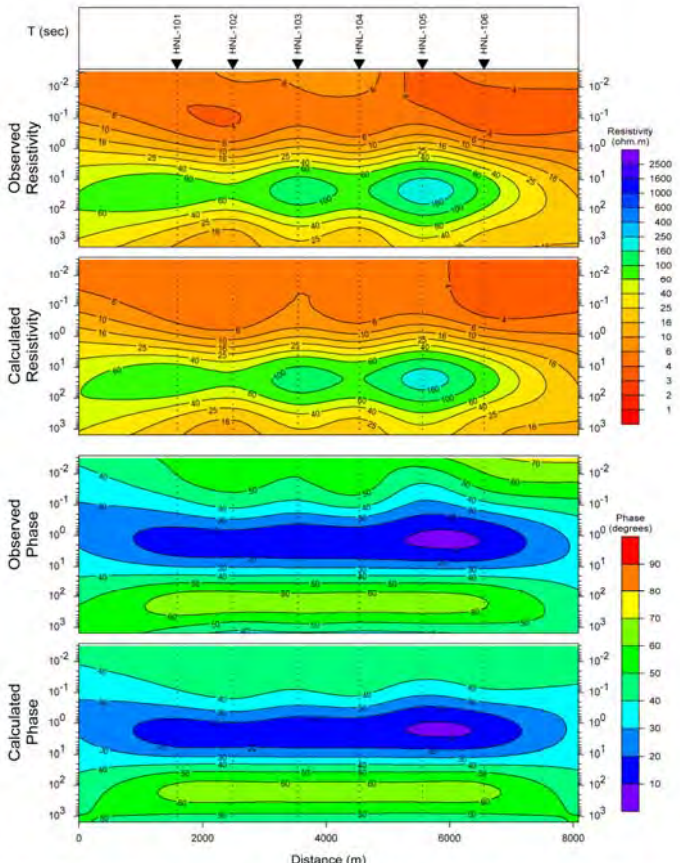

Pseudo Section of Apparent Resistivity and Phase Difference (HNL100)

(Upper: TE mode, Lower: TM mode)

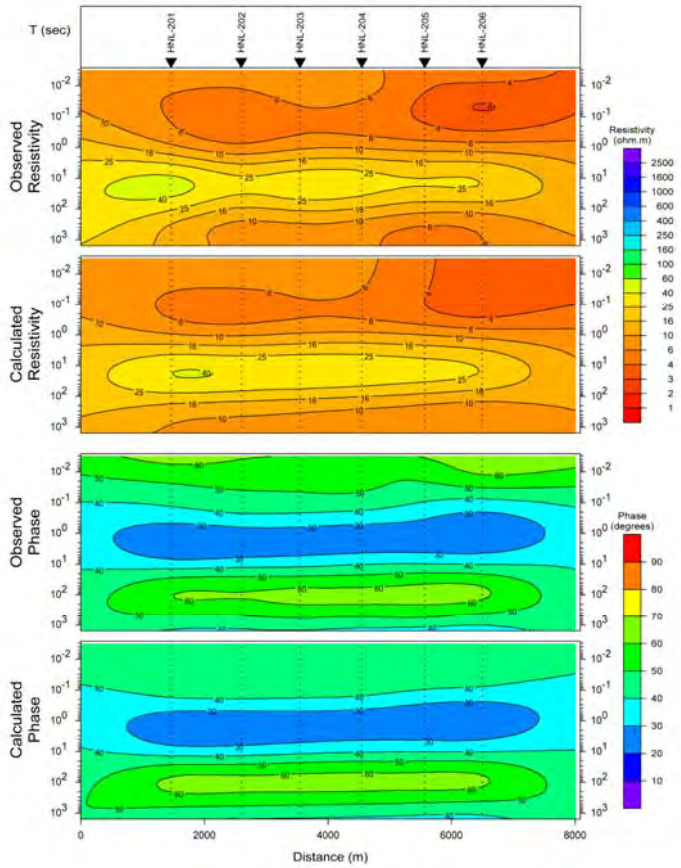

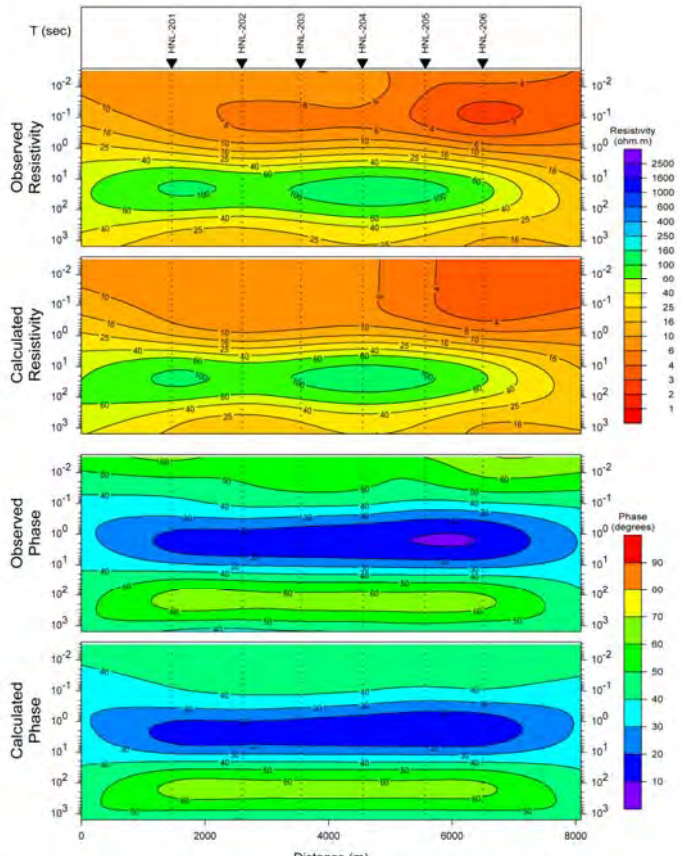

Pseudo Section of Apparent Resistivity and Phase Difference (HNL200)

(Upper: TE mode, Lower: TM mode)

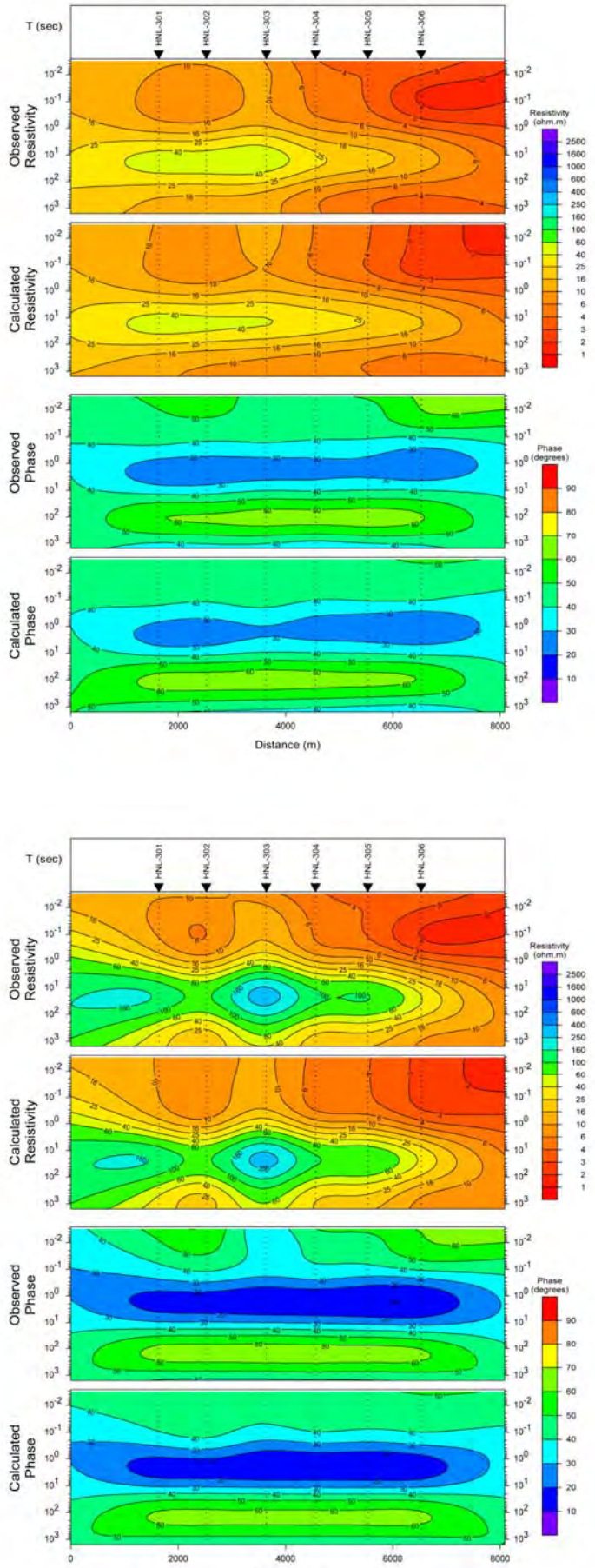

Pseudo Section of Apparent Resistivity and Phase Difference (HNL300)

(Upper: TE mode, Lower: TM mode)

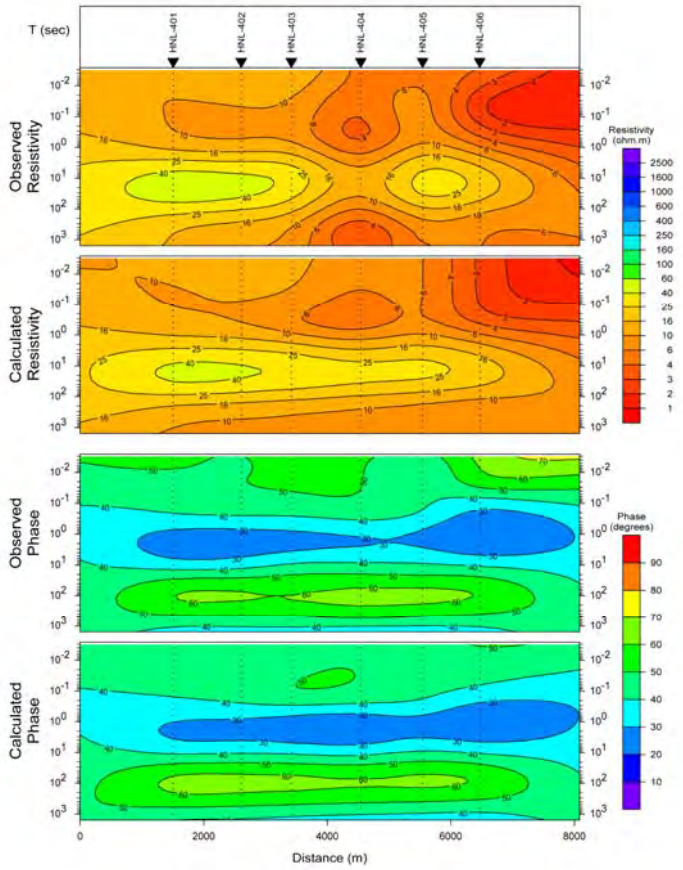

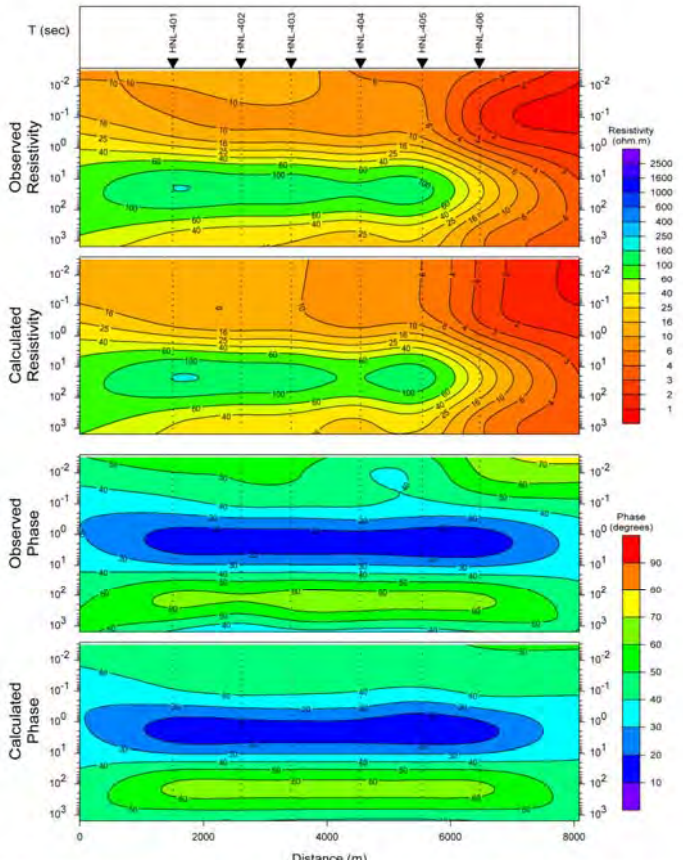

Pseudo Section of Apparent Resistivity and Phase Difference (HNL400)

(Upper: TE mode, Lower: TM mode)

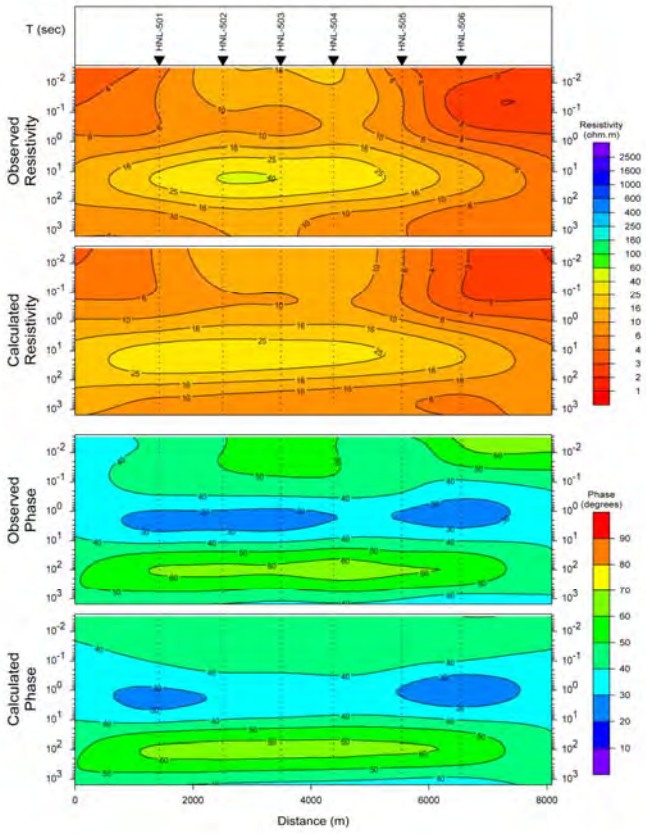

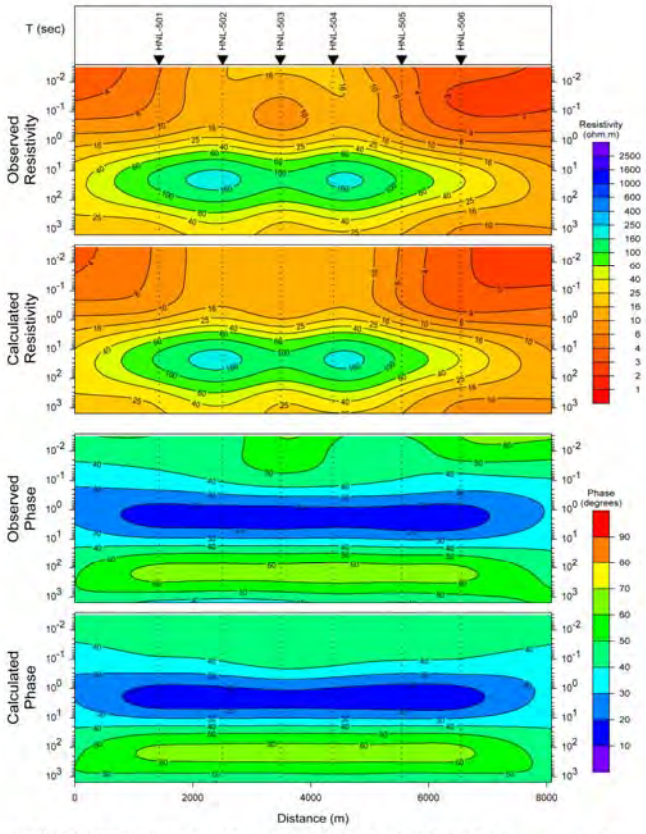

Pseudo Section of Apparent Resistivity and Phase Difference (HNL500)

(Upper: TE mode, Lower: TM mode)

Appendix-5 Preliminary Economic Analysis

A. Case-1: Plant Factor 80%, Well successful rate 60%

A.1 Investment schedule

Investment Schedule

Project Description								
Name	Hanle GPP							
Installed capacity	15	MW						
Plant factor	80	%						
Station use	9	%						
Generated energy	105.1	GWh						
Saled energy	95.7	GWh						
Costruction cost	104.5	M$	(2015 price)					
Construction period	5	years	(2016-2020)					
Operating period	30	years	(2021-2050)					

Captital cost disbursement schedule (2015 price, in US$ million)

Period		1	2	3	4	5	Total
Year		2016	2017	2018	2019	2020	
1. Test drilling		4.2	4.2				8.4
2. Preparatory works			2.5				2.5
3. Main works							
Consulting fees (design)			2.4				2.4
Production well drilling				15.0	20.0	15.0	49.9
Steam gathering system (FCRC)				1.8	2.4	1.8	6.0
Plant costruction				7.4	9.9	7.4	24.8
Consulting fees (supervision)				1.0	1.3	1.0	3.2
Administration & management				1.0	1.3	1.0	3.2
Physical contingencies				1.2	1.6	1.2	4.0
Total		4.2	9.1	27.4	36.5	27.4	104.5
Inflation	US$ inflation	2%	2%	2%	2%	2%	
	Inflation factor (base is 2015)	1.020	1.040	1.061	1.082	1.104	

Captital cost disbursement schedule (nominal price, in US$ million)

Period	1	2	3	4	5	Total
Year	2016	2017	2018	2019	2020	
1. Test drilling	4.3	4.4				8.7
2. Preparatory works		2.6				2.6
3. Main works						
Consulting fees (design)		2.5				2.5
Production well drilling			15.9	21.6	16.5	54.0
Steam gathering system (FCRC)			1.9	2.6	2.0	6.5
Plant costruction			7.9	10.7	8.2	26.8
Consulting fees (supervision)			1.0	1.4	1.1	3.5
Administration & management			1.0	1.4	1.1	3.5
Physical contingencies			1.3	1.7	1.3	4.4
Total	4.3	9.5	29.0	39.5	30.2	112.5

A.2 Financing plan

Financing Plan

Funding Sources and Financing Terms

Source	Interest	Repayment period (yr)	Grace period (yr)	Commitment fee	Front-end fee
Equity capital (Equity)					
ODA grant fund (grant)					
Government budget (GoD)					
ODA loan-mulitlateral (ODA-Mul)	5.0%	20	5	1.0%	1.0%
ODA loan-bilateral (ODA-Bi)	2.5%	30	10	0.5%	0.0%
Commercial bank loan (CB)	6.0%	10	3	1.0%	1.0%

Breakdown of Base Costs and Financing Plan (in US$ million)

Year	Grant	GoE	ODA-Mul	ODA-Bi	CB	Equity	Total
1. Test drilling	4.3	4.4					8.7
2. Preparatory works		2.6					2.6
3. Main works							
Consulting fees (design)		2.5					2.5
Production well drilling					41.6	12.4	54.0
Steam gathering system (FCRC)					5.0	1.5	6.5
Plant costruction					20.7	6.2	26.8
Consulting fees (supervision)						3.5	3.5
Administration & management						3.5	3.5
Physical contingencies						4.4	4.4
Total	4.3	9.5			67.3	31.5	112.5

Financial Costs during Construction (in US$ million)

Year	2016	2017	2018	2019	2020	Total
1. ODA grant fund	4.3	4.4				8.7
2. Government budget		5.1				5.1
3. Equity capital			9.2	12.6	9.6	31.5
4. ODA loan-multilateral						
Disbursement						
Interest						
Sub-total						
5. ODA loan-bilateral						
Disbursement						
Interest						
Sub-total						
6. Commercial bank loan						
Disbursement			19.8	26.9	20.6	67.3
Interest				1.2	2.8	4.0
Sub-total			19.8	28.1	23.4	71.3
Total of 1 through 6	4.3	9.5	29.0	40.7	33.0	116.5
7. Front-end fee						
ODA loan-multilateral						
ODA loan-bilateral						
Commercial bank loan		0.7				0.7
Total		0.7				0.7
8. Commitment fee						
ODA loan-multilateral						
ODA loan-bilateral						
Commercial bank loan			0.5	0.2	0.0	0.7
Total			0.5	0.2	0.0	0.7
Total of 1 through 8	4.3	10.2	29.5	40.9	33.0	117.9
					Loan ratio	69.8%

A.3 Assumptions on Financial Analysis

Assumptions on Financial Analysis

Loan profile	Loan amount (M$)	Interest	Loan repay period (yr)	Grace period (yr)	Principal repay period (yr)
ODA loan - multilateral	0.0	5.0%	20	5	15
ODA loan - bilateral	0.0	2.5%	30	10	20
Commercial bank (CB)	72.7	6.0%	10	3	7
Total	72.7				
Equity capital	31.5	M$			
Fixed assets					
GoD	13.8	M$	(to be transferred to IPP)		
IPP	104.2	M$			
Energy sale					
Saled energy	95.7	GWh			
Sales price (2015 price)	16.10	¢/kWh			
Sales price (in 2021)	18.13	¢/kWh			
Escalation rate (/yr)	2.0%				
Operation & maintenance cost					
O&M cost (2015 price)	1.6	M$ (1.5% of capital cost)			
O&M cost (in 2021)	1.8	M$ (1.5% of capital cost)			
Escalation rate (/yr)	2.0%				
Depreciation					
Asset value (US$ million)	117.9	(including GoE assets)			
Useful life (in year)	30				
Residual value	0%				
Method	Straight line				
Concession fee	5.0%	of sales revenue			
Escrow account (for CB loan)	50.0%	of annual debt service			
Cash required	2.0%	of sales revenue			
Accounts receivable	12.5%	1.5 month of sales revenue			
Accounts payable	8.0%	1 month of O&M cost			
Deposite rate	3.0%				
Income tax	30.0%	from 8th year of operation			
Dividend rate	70.0%	of net profit			
Exchanger rate					

A.4 Graphs

Period	-5	-4	-3	-2	-1	1	2	3	4	5	6	7	8	9	10	11	12	13	14	15	16	17	18	19	20	21	22	23	24	25	26	27	28	29	30
Year	2016	2017	2018	2019	2020	2021	2022	2023	2024	2025	2026	2027	2028	2029	2030	2031	2032	2033	2034	2035	2036	2037	2038	2039	2040	2041	2042	2043	2044	2045	2046	2047	2048	2049	2050
Capital cost	-4.3	-10.2	-29.5	-40.9	-33.0																														
Revenue						17.3	17.7	18.0	18.4	18.8	19.1	19.5	19.9	20.3	20.7	21.1	21.6	22.0	22.4	22.9	23.3	23.8	24.3	24.8	25.3	25.8	26.3	26.8	27.4	27.9	28.5	29.0	29.6	30.2	30.8
Make up wells						0.0	0.0	0.0	0.0	0.0	0.0	0.0	0.0	0.0	7.9	0.0	0.0	0.0	0.0	0.0	0.0	0.0	0.0	0.0	7.9	0.0	0.0	0.0	0.0	0.0	0.0	0.0	0.0	0.0	7.9
O&M costs						1.8	1.8	1.8	1.9	1.9	1.9	2.0	2.0	2.1	2.1	2.2	2.2	2.2	2.3	2.3	2.4	2.4	2.5	2.5	2.6	2.6	2.7	2.7	2.8	2.8	2.9	3.0	3.0	3.1	3.1
Concession fee						0.9	0.9	0.9	0.9	0.9	1.0	1.0	1.0	1.0	1.0	1.1	1.1	1.1	1.1	1.1	1.2	1.2	1.2	1.2	1.3	1.3	1.3	1.3	1.4	1.4	1.4	1.5	1.5	1.5	1.5
Debt service						14.8	14.1	13.5	12.9	12.3	11.6	11.0	0.0	0.0	0.0	0.0	0.0	0.0	0.0	0.0	0.0	0.0	0.0	0.0	0.0	0.0	0.0	0.0	0.0	0.0	0.0	0.0	0.0	0.0	0.0
Tax						0.0	0.0	0.0	0.0	0.0	0.0	0.0	3.7	3.8	1.6	4.1	4.3	4.5	4.7	4.8	5.0	5.2	5.4	5.6	3.4	6.0	6.2	6.4	6.6	6.8	7.0	7.2	7.5	7.7	5.6
Surplus						▲ 0.0	0.9	1.8	2.7	3.7	4.6	5.6	13.2	13.4	8.1	13.8	14.0	14.2	14.4	14.6	14.8	15.0	15.2	15.4	10.1	15.9	16.1	16.4	16.6	16.9	17.1	17.4	17.6	17.9	12.6

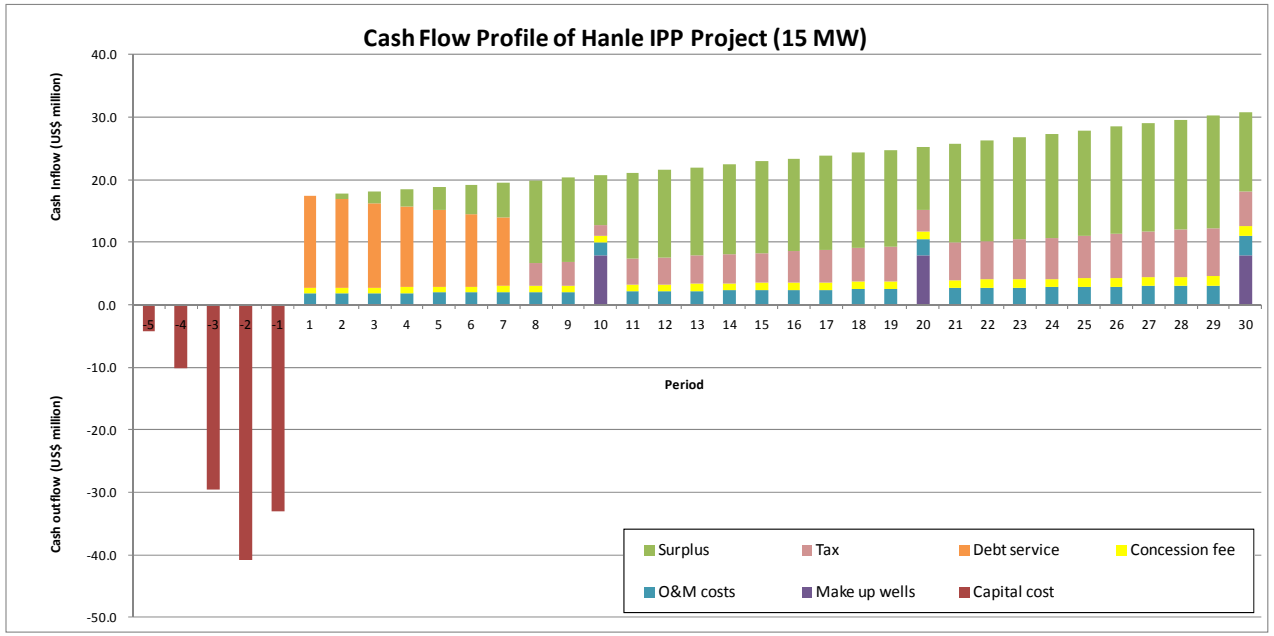

B. Case-2: Plant Factor 80%, Well successful rate 70%

B.1 Investment schedule

Investment Schedule

Project Description								
Name	Hanle GPP							
Installed capacity	15	MW						
Plant factor	80	%						
Station use	9	%						
Generated energy	105.1	GWh						
Saled energy	95.7	GWh						
Costruction cost	98.4	M$	(2015 price)					
Construction period	5	years	(2016-2020)					
Operating period	30	years	(2021-2050)					

Captital cost disbursement schedule (2015 price, in US$ million)

Period		1	2	3	4	5	Total
Year		2016	2017	2018	2019	2020	
1. Test drilling		4.2	4.2				8.4
2. Preparatory works			2.5				2.5
3. Main works							
Consulting fees (design)			2.3				2.3
Production well drilling				13.4	17.8	13.4	44.6
Steam gathering system (FCRC)				1.8	2.4	1.8	6.0
Plant costruction				7.4	9.9	7.4	24.8
Consulting fees (supervision)				0.9	1.2	0.9	3.0
Administration & management				0.9	1.2	0.9	3.0
Physical contingencies				1.1	1.5	1.1	3.8
Total		4.2	9.0	25.6	34.1	25.6	98.4
Inflation	US$ inflation	2%	2%	2%	2%	2%	
	Inflation factor (base is 2015)	1.020	1.040	1.061	1.082	1.104	

Captital cost disbursement schedule (nominal price, in US$ million)

Period	1	2	3	4	5	Total
Year	2016	2017	2018	2019	2020	
1. Test drilling	4.3	4.4				8.7
2. Preparatory works		2.6				2.6
3. Main works						
Consulting fees (design)		2.4				2.4
Production well drilling			14.2	19.3	14.8	48.3
Steam gathering system (FCRC)			1.9	2.6	2.0	6.5
Plant costruction			7.9	10.7	8.2	26.8
Consulting fees (supervision)			1.0	1.3	1.0	3.3
Administration & management			1.0	1.3	1.0	3.3
Physical contingencies			1.2	1.6	1.2	4.1
Total	4.3	9.3	27.1	36.9	28.2	105.8

B.2 Financing plan

Financing Plan

Funding Sources and Financing Terms

Source	Interest	Repayment period (yr)	Grace period (yr)	Commitment fee	Front-end fee
Equity capital (Equity)					
ODA grant fund (grant)					
Government budget (GoD)					
ODA loan-mulitlateral (ODA-Mul)	5.0%	20	5	1.0%	1.0%
ODA loan-bilateral (ODA-Bi)	2.5%	30	10	0.5%	0.0%
Commercial bank loan (CB)	6.0%	10	3	1.0%	1.0%

Breakdown of Base Costs and Financing Plan (in US$ million)

Year	Grant	GoE	ODA-Mul	ODA-Bi	CB	Equity	Total
1. Test drilling	4.3	4.4					8.7
2. Preparatory works		2.6					2.6
3. Main works							
Consulting fees (design)		2.4					2.4
Production well drilling					37.2	11.1	48.3
Steam gathering system (FCRC)					5.0	1.5	6.5
Plant costruction					20.7	6.2	26.8
Consulting fees (supervision)						3.3	3.3
Administration & management						3.3	3.3
Physical contingencies						4.1	4.1
Total	4.3	9.3			62.9	29.4	105.8

Financial Costs during Construction (in US$ million)

Year	2016	2017	2018	2019	2020	Total
1. ODA grant fund	4.3	4.4				8.7
2. Government budget		5.0				5.0
3. Equity capital			8.6	11.8	9.0	29.4
4. ODA loan-multilateral						
Disbursement						
Interest						
Sub-total						
5. ODA loan-bilateral						
Disbursement						
Interest						
Sub-total						
6. Commercial bank loan						
Disbursement			18.5	25.1	19.2	62.9
Interest				1.1	2.6	3.7
Sub-total			18.5	26.2	21.8	66.6
Total of 1 through 6	4.3	9.3	27.1	38.0	30.8	109.6
7. Front-end fee						
ODA loan-multilateral						
ODA loan-bilateral						
Commercial bank loan		0.7				0.7
Total		0.7				0.7
8. Commitment fee						
ODA loan-multilateral						
ODA loan-bilateral						
Commercial bank loan			0.5	0.2	0.0	0.7
Total			0.5	0.2	0.0	0.7
Total of 1 through 8	4.3	10.0	27.6	38.2	30.8	110.9
					Loan ratio	69.8%

B.3 Assumptions on Financial Analysis

Assumptions on Financial Analysis

Loan profile	Loan amount (M$)	Interest	Loan repay period (yr)	Grace period (yr)	Principal repay period (yr)
ODA loan - multilateral	0.0	5.0%	20	5	15
ODA loan - bilateral	0.0	2.5%	30	10	20
Commercial bank (CB)	67.9	6.0%	10	3	7
Total	67.9				
Equity capital	29.4	M$			
Fixed assets					
GoD	13.6	M$	(to be transferred to IPP)		
IPP	97.3	M$			
Energy sale					
Saled energy	95.7	GWh			
Sales price (2015 price)	15.10	¢/kWh			
Sales price (in 2021)	17.01	¢/kWh			
Escalation rate (/yr)	2.0%				
Operation & maintenance cost					
O&M cost (2015 price)	1.5	M$ (1.5% of capital cost)			
O&M cost (in 2021)	1.7	M$ (1.5% of capital cost)			
Escalation rate (/yr)	2.0%				
Depreciation					
Asset value (US$ million)	110.9	(including GoE assets)			
Useful life (in year)	30				
Residual value	0%				
Method	Straight line				
Concession fee	5.0%	of sales revenue			
Escrow account (for CB loan)	50.0%	of annual debt service			
Cash required	2.0%	of sales revenue			
Accounts receivable	12.5%	1.5 month of sales revenue			
Accounts payable	8.0%	1 month of O&M cost			
Deposite rate	3.0%				
Income tax	30.0%	from 8th year of operation			
Dividend rate	70.0%	of net profit			
Exchanger rate					

B.4 Graphs

Period	-5	-4	-3	-2	-1	1	2	3	4	5	6	7	8	9	10	11	12	13	14	15	16	17	18	19	20	21	22	23	24	25	26	27	28	29	30
Year	2016	2017	2018	2019	2020	2021	2022	2023	2024	2025	2026	2027	2028	2029	2030	2031	2032	2033	2034	2035	2036	2037	2038	2039	2040	2041	2042	2043	2044	2045	2046	2047	2048	2049	2050
Capital cost	-4.3	-10.0	-27.6	-38.2	-30.8																														
Revenue						16.3	16.6	16.9	17.3	17.6	18.0	18.3	18.7	19.1	19.4	19.8	20.2	20.6	21.0	21.5	21.9	22.3	22.8	23.2	23.7	24.2	24.7	25.1	25.7	26.2	26.7	27.2	27.8	28.3	28.9
Make up wells						0.0	0.0	0.0	0.0	0.0	0.0	0.0	0.0	0.0	7.9	0.0	0.0	0.0	0.0	0.0	0.0	0.0	0.0	0.0	7.9	0.0	0.0	0.0	0.0	0.0	0.0	0.0	0.0	0.0	7.9
O&M costs						1.7	1.7	1.7	1.8	1.8	1.8	1.9	1.9	1.9	2.0	2.0	2.1	2.1	2.1	2.2	2.2	2.3	2.3	2.4	2.4	2.5	2.5	2.6	2.6	2.7	2.7	2.8	2.8	2.9	3.0
Concession fee						0.8	0.8	0.8	0.9	0.9	0.9	0.9	0.9	1.0	1.0	1.0	1.0	1.0	1.1	1.1	1.1	1.1	1.1	1.2	1.2	1.2	1.2	1.3	1.3	1.3	1.3	1.4	1.4	1.4	1.4
Debt service						13.8	13.2	12.6	12.0	11.5	10.9	10.3	0.0	0.0	0.0	0.0	0.0	0.0	0.0	0.0	0.0	0.0	0.0	0.0	0.0	0.0	0.0	0.0	0.0	0.0	0.0	0.0	0.0	0.0	0.0
Tax						0.0	0.0	0.0	0.0	0.0	0.0	0.0	3.4	3.6	1.4	3.9	4.0	4.2	4.4	4.5	4.7	4.9	5.1	5.2	3.1	5.6	5.8	6.0	6.2	6.4	6.6	6.8	7.0	7.2	5.1
Surplus						0.0	0.9	1.7	2.6	3.5	4.4	5.2	12.4	12.6	7.2	12.9	13.1	13.3	13.5	13.7	13.9	14.1	14.3	14.5	9.1	14.9	15.1	15.3	15.6	15.8	16.0	16.3	16.5	16.8	11.5

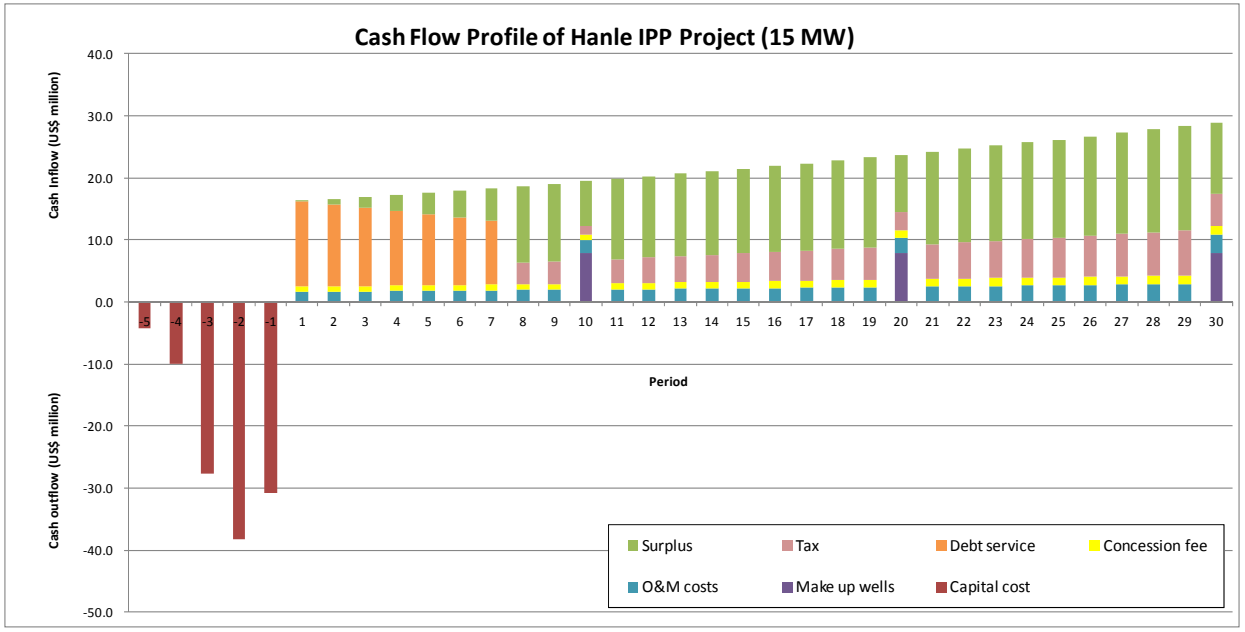

C. Transmission Cost per kWh

plant factor	80%	15.0 MW	8760		
New Transmission Line Length	70	km			
Construction Cost	17.5	mil $	Interest Rate	10	%
Capital Recovery Factor (10%, 30 years)	10.6	%	Economic Life	30	year
Annualized Capital Cost	1.9	mil $/year			
Produced Energy (Plant)	105.12	GWh			
Station Use	9.0	%	95.659		
Transmission Loss	8.6	%	87.433		
Energy Sales	87.4	GWh			
Transmission Cost	**0.021**	¢/kWh			

Appendix-6 Volumetric Calculation Method

PROCEEDINGS, Thirty-Ninth Workshop on Geothermal energy Reservoir Engineering
Stanford University, Stanford, California, January 26-28, 2015
SGP-TR-204

A Rational and Practical Calculation Approach for Volumetric Method

Shinya Takahashi, Satoshi Yoshida

Nippon Koei, Co., Ltd, 5-4 Kojimachi, Chiyoda-ku, Tokyo 102-8539, Japan

TAKAHASHI-SH@n-koei.jp, YOSHIDA-ST@n-koei.jp

Keywords: volumetric method, typical power cycle process, steam-liquid separation process, adiabatic heat drop, exergy efficiency, available thermal energy function

ABSTRACT

The USGS volumetric method together with Monte Carlo simulations is widely used for assessing the electrical capacity of a geothermal reservoir. However, the USGS method appears not to be easily usable with the probabilistic method. On the other hand, some of prevailing references practice the volumetric method calculations differently from the USGS method; in many cases rational explanations are not necessarily provided. Instead, we herein propose a rational and practical calculation method by reflecting both the steam-liquid separation process at separator and the adiabatic heat-drop process at turbine, together with a rational temperature at condenser; that can be used with Monte Carlo method also. The proposed method enables us to assess electrical capacity by clearly and rationally defined parameters for the equations; resulting in clearer understandings of the electrical capacity estimation of a geothermal reservoir. The proposed method shows an approximate agreement with the USGS method, but gives larger estimation results than the ones given by the prevailing calculation method. This might be attributed to how underground-related parameters should be estimated.

1. INTRODUCTION

USGS (Muffler, L.J.P, Editor 1978) introduced the stored heat method for assessing the electrical capacity of a geothermal reservoir. The equations for the methods are as follows.

$$q_r = \rho C V (T_r - T_{ref}) \quad \text{[kJ]} \quad (1)$$

$$R_g = q_{WH} / q_r \quad \text{[-]} \quad (2)$$

$$q_{WH} = m_{WH} (h_{WH} - h_{ref}) \quad \text{[kJ]} \quad (3)$$

$$W_A = m_{WH} \left[h_{WH} - h_0 - T_0 (s_{WH} - s_0) \right] \quad \text{[kJ] or [kW]} \quad (4)$$

(for a geothermal reservoir temperature > 150°C)

$$E = W_A \eta_u / (FL) \quad \text{[kJ/s] or [kW]} \quad (5)$$

Where q_r is reservoir geothermal energy, q_{WH} is geothermal energy recovered at wellhead, T_r is reservoir temperature, T_{ref} is reference temperature, T_0 is rejection temperature (Kelvin), m_{WH} is mass of geothermal fluid produced at wellhead, h_{WH} is specific enthalpy of geothermal fluid produced at wellhead, h_{ref} is specific enthalpy of geothermal fluid at reference temperature, h_0 is specific enthalpy of fluid at final state, s_{WH} is specific entropy of fluid at wellhead, s_0 is specific entropy of fluid at final state, ρC is volumetric specific heat of reservoir, V is reservoir volume, Rg is recovery factor, W_A is available work (exergy), E is power plant capacity, η_u is utilization factor (that includes energy ratio of steam fraction separated from the fluid and exergy efficiency), F is power plant capacity factor and L is power plant life.

While it is said that this is a good approach from theoretical perspectives, it includes issues to be discussed when used for liquid dominant geothermal fluid recovered at wellhead.

S K. Garg et al (2011) pointed out that the “available work” of USGS methodology is a strong function of the reference temperature, and that the utilization factor (i.e. ratio of electric energy generated to available work) depends on both power generating system and reference temperature. On the other hand, the AGEG Geothermal energy Lexicon (compiled by J. Lawless 2010) described that recovery factor of the USGS method rejects both the fraction of heat below commercially useful temperature and fraction of unrecoverable heat, when used for liquid dominant geothermal fluid. These and other relevant references we reviewed suggest that we should examine utilization factor and/or recovery factor in connection with both of liquid-steam separation process and reference temperature when we use the USGS method for a flash type power cycle using liquid dominant geothermal fluid. The determination of these parameters with considerations on the relations among these, will require proper and deep understandings of geothermal generation system. In addition, we observe that the equation (1) to (4) appear to be imbalancing, because the equations (1) to (3) include two reference-related parameters (T_{ref}, h_{ref}) whereas the exergy equation (4) does not include reference-related parameters in the square bracket. We also observe that the calculations using the USGS equations that include variable T_r dependent-parameters (h_{WH}, s_{HW}), with

Monte Carlo simulations, would be laborious. Thus, we consider that the USGS method would not be easily applicable for assessment of electric capacity of a geothermal reservoir with Monte Carlo simulations.

In place of the USGS method, the different method is being used by many prevailing references for geothermal resource estimations. We name this different method "the prevailing method". The equation of the prevailing method is given as follows.

$$E = R_g \eta_c \rho C V (T_r - T_{ref}) / (FL) \qquad \text{[kJ/s] or [kW]} \qquad (6)$$

Where η_c is named as "conversion factor".

The core term $\rho CV(T_r - T_{ref})$ in the equation (6) is exactly the same as the equation (1) of the USGS method. The theoretical concept, however, appears to be quite different. The prevailing method adopts much higher temperatures such as 150 ºC, 180 ºC or others to the reference temperature (T_{ref}); while the USGS method defines that the reference temperature (T_{ref}) for all cycles is chosen as 15 ºC (i.e. the average ambient temperature of the USA) and the rejection temperature as T_0=40 ºC (i.e. a typical condenser temperature) in the calculation of available work (W_A) of the equation (4). The reference temperature in the prevailing method is sometimes named as the abandonment temperature.

The prevailing method is said to be derived from Pálmason, G. *et al* (1985, in Icelandic). There seems however to have been variations in slecting the temperature (AGEG, 2010 refers to various cases). It is explained sometimes in such a way that it adopts a separator temperature to the reference temperature to exclude the geothermal energy to be abandoned as liquid form that is separated from fluid at separator. Here, a question arises on how the equation distinguishes the steam and the liquid; both separated in the separator at the same temperature; thereafter the liquid is to be abandoned whereas the steam to be used. Another application is that a cut-off temperature is sometimes selected. It would be conceived that the cut-off temperature is included in the equations to exclude non-economically-valuable fluid produced from the reservoir that has already been delineated by practitioners, where the cut-off temperature is understood as the one that defines the outer limit of the reservoir. Here, another question arises on why the cut-off temperature should be included in the equation if the outer limit of the reservoir has already been defined by the cut-off temperature to exclude non-economically-valuable fluid. Both cases above seem to be illogical.

The other different point is that the prevailing method adopts the conversion factor η_c ranging from 0.13 to 0.16 approximately; while the USGS method recommends 0.4-0.45 to the utilization factor η_u defined by the equation (5). *Obiter,* the equation (6) appears to be nothing but expressing a thermodynamic process: the term $R_g\rho CV(T_r - T_{ref})$, ($T_r$ >0 ºC and T_{ref}>0 ºC are assumed here), is the recovered heat energy that is made available when the temperature of fluid changes from T_r to T_{ref}, the fluid that conveys the heat from the reservoir. The term $R_g\rho CV(T_r - T_{ref})$ in the equation (1) of the USGS method expresses the heat energy available at the temperature condition of T_{ref}; in this context, it is clear that the utilization factor η_u was intended to include the steam energy ratio against the recovered energy and the exergy efficiency. On the other hand, it appears not to be clear what efficiencies are included in the conversion factor η_c because inclusion of the T_{ref} of much higher temperature in the equation (6) makes the thermodynamic implication of the equation ambiguous.

Thus, we consider that the prevailing method might be an empirical method based on field wisdom that attempts to assess electric capacity of geothermal reservoir that produces liquid dominate fluid at wellhead by modifying the concept of the USGS method. This is further discussed in the section 6 of this paper.

Instead, we herein propose a rational and practical method that defines the aboveground-related key parameters; that reflects the steam-liquid separation process in the calculations; that can be used with the Monte Carlo method also. The proposed method enables us to select a reference temperature, a recovery factor and a conversion/utilization factor rationally and independently, and separately from consideration of the steam-liquid separation process; that results in clearer understanding of the resource estimation.

2. INTRODUCTION OF AVAILABLE THERMAL ENERGY FUNCTION ζ

We begin our explanation with turbine side; because our primary interest lies on electrical power generation, and for that reason here includes the key point of this paper. We calculate electric energy by using the adiabatic heat-drop concept (or exergy concept) at turbine. This is widely used for design of turbine-generator system. In Figure-1 we illustrated the conceptual model of geothermal generation system we assumed. The electric capacity produced at turbine-generator system is written as;

$$E = \eta_{ex} m_{tb_{in}} (h_{tb_{in}} - h_{tb_{out}}) / (FL) \qquad \text{[kW]} \qquad (7)$$

or

$$E = \eta_{ex} (q_{tb_{in}} - q_{tb_{out}}) / (FL) \qquad \text{[kW]} \qquad (8)$$

Where η_{ex} is exergy efficiency, $m_{tb\ in}$ is mass of steam at inlet of turbine, $h_{tb\ in}$ is specific enthalpy at inlet of turbine, $h_{tb\ out}$ is specific enthalpy at outlet of turbine, $q_{tb\ in}$ is thermal energy at inlet of turbine, $q_{tb\ out}$ is thermal energy immediately after turbine.

Here, we introduce the "available thermal energy function" defined by the following equation.

$$\zeta = (q_{tb_{in}} - q_{tb_{out}}) / q_{WH} \qquad \text{[-]} \qquad (9)$$

Where ζ is the available thermal energy function.

The available thermal energy function (9) we introduced, represents the ratio of the heat-drop at turbine against thermal energy available at wellhead. In other word, it represents the ratio of available thermal energy for electrical power generation against thermal energy available at wellhead.

Combined with the available thermal energy function (9), the equation (8) is rewritten as;

$$E = \eta_{ex}\zeta q_{WH}/(FL) \quad \text{[kW]} \quad (10)$$

Further, combined with the equations (1) and (2), the equation (10) is rewritten as;

$$E = \eta_{ex}\zeta R_g \rho C V (T_r - T_{ref})/(FL) \quad \text{[kW]} \quad (11)$$

where

$$\rho C = (1-\varphi)C_r\rho_r + \varphi C_f \rho_f \quad \text{[kJ/(kg°C)]} \quad (12)$$

Where C_r is specific heat of reservoir rock matrix, C_f is specific heat of reservoir fluid, ρ_r is density of reservoir rock matrix and ρ_f is density of reservoir fluid.

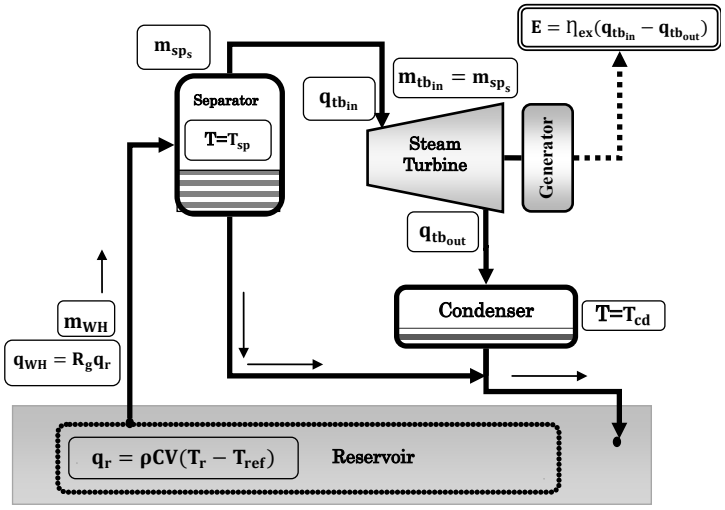

Figure 1 Simplified single flash power plant schematic

The available thermal energy function ζ in the equation (11) exclusively includes the thermal energy of the steam fraction only that is used for power generation. By introducing the available thermal energy function ζ to the volumetric method calculation, we can limit our considerations about utilization factor or conversion factor to turbine-generator related matters; and we can also limit our considerations about recovery factor to underground phenomenon. Thereby, the proposed method enables a rational assessment of electrical capacity of a geothermal reservoir by rationally defined parameters of the equations of the volumetric method.

3. INTRODUCTION OF READILY CALCULABLE EQUATIONS FOR ζ

In this section, we will describe the procedure of how we obtain calculable equations of the available thermal energy function ζ; and thereafter, we will introduce approximation equations of the available thermal energy function ζ for practical uses, as direct functions of a reservoir temperature T_r.

3.1 Assumptions

We assume that geothermal energy is recovered as saturated and single-phase liquid. This is not only for a simplification of calculation; but also for a reason that S. K. Sanyal et al (2005) pointed out that the "explicit consideration of the two-phase volume in reservoir estimation is not critical".

We also assume a single flash power cycle with a separator of a typical pressure. Dry steam is assumed at inlet of turbine; wet steam is then assumed immediately after turbine to obtain near-realistic power output. We will assign a typical temperature to condenser, too.

3.2 Determination of "available thermal energy function ζ"

3.2.1 Geothermal energy recovered at the wellhead (q_{WH})

The geothermal energy recovered at wellhead is defined by the equation (3) when the final state of the fluid is the one under the ambient condition. However, since we assume a geothermal power plant of single flash type, the final state of the fluid contributing power generation should be under the condenser condition. We will assume at a later part of this paper the condenser temperature. Thus, at this step of calculation we assume that all the recovered heat at the well head will be sent from the wellhead to the separator.

$$q_{WH_L} = m_{WH_L} h_{WH_L} \quad \text{[kJ]} \quad (13)$$

Where $q_{WH\,L}$ is geothermal energy recovered as liquid phase at wellhead, $m_{WH\,L}$ is mass of single phase geothermal liquid produced at wellhead, $h_{WH\,L}$ is specific enthalpy of single phase geothermal liquid produced at wellhead.

3.2.2 Thermal energy at the inlet of the turbine ($q_{tb_{in}}$)

The thermal energy at turbine inlet ($q_{tb_{in}}$) should be the thermal energy of dry steam separated at separator from fluid recovered at wellhead. The following equations give the mass of the steam fraction separated at separator, and to be sent to turbine.

$$m_{sp_S} = \alpha_{sp_S} m_{WH_L} \quad \text{[kg]} \quad (14)$$

$$\alpha_{sp_S} = (h_{WH_L} - h_{sp_L}) / (h_{sp_S} - h_{sp_L}) \quad \text{[-]} \quad (15)$$

Where $m_{sp\,s}$ is mass of steam fraction separated at separator, $\alpha_{sp\,s}$ is ratio of steam mass fraction separated at separator, $h_{sp\,L}$ is specific enthalpy of liquid fraction separated at separator, and $h_{sp\,S}$ is specific enthalpy of steam fraction separated at separator.

From the above, the thermal energy at turbine inlet is given by;

$$q_{tbin} = m_{sp_S} h_{sp_S} = \alpha_{sp_S} m_{WH_L} h_{sp_S} \quad \text{[kJ]} \quad (16)$$

3.2.3 Thermal energy immediately after the turbine($q_{tb_{out}}$)

The dry steam in turbine is losing its thermal energy; and becomes wet steam when exhausted from turbine. The adiabatic heat-drop concepts explains this process. The following equation gives the dryness (quality) of the wet steam immediately after turbine.

$$\chi = (s_{sp_S} - s_{cd_L}) / (s_{cd_s} - s_{cd_L}) \quad \text{[-]} \quad (17)$$

Where χ is quality of steam (dryness of steam), $S_{sp\,S}$ is entropy of steam fraction at separator, $S_{cd\,L}$ is entropy of liquid fraction at condenser and $S_{cd\,S}$ is entropy of steam fraction at condenser.

Then the enthalpy of the wet steam is given by;

$$h_{tbout_{SL}} = h_{cd_L} + (h_{cd_S} - h_{cd_L})\chi \quad \text{[kJ/kg]} \quad (18)$$

Where $h_{tbout\,SL}$ is specific enthalpy of wet steam immediately after turbine, $h_{cd\,L}$ is specific enthalpy of liquid fraction at condenser and $h_{cd\,S}$ is specific enthalpy of steam fraction at condenser.

Since the same mass as that of the dry steam is exhausted out of turbine, the thermal energy immediately after turbine is given by;

$$q_{tb_{out}} = m_{sp_S} h_{tb_{out_{SL}}} = \alpha_{sp_S} m_{WH_L} h_{tb_{out_{SL}}} \quad \text{[kJ]} \quad (19)$$

3.2.3 The available thermal energy function ζ

Replacing the variables of the equation (9) with the equations (13), (16), and (19) gives the following equation.

$$\zeta = \alpha_{sp_S} (h_{sp_S} - h_{tb_{out_{SL}}}) / (h_{WH_L}) \quad \text{[-]} \quad (20)$$

With the equation above, we can obtain specific values of the ζ by giving the enthalpies.

3.2.3 Introduction of approximation equations of ζ for practical uses.

Calculation using the variables in the equation (20) for each reservoir temperature is laborious and not readily usable with the Monte Carlo Method. We will then introduce approximation equations of the ζ from the calculation results of the five typical reservoir temperatures, i.e. 180 ºC, 200 ºC, 250 ºC, 300 ºC, and 340 ºC.

For the calculation we assume that the separator pressure is 5 bar (151.8 ºC), because the produced electrical power would be maximum when the separator pressure is around 4 bar to 5 bar. Let us assume the power generation is E=1.00 when the separator temperature is 150 ºC. A simplified calculation for various separator temperatures gives the following results: i.e. when the separator temperature is

120 ºC, 140 ºC, 160 ºC, and 180 ºC; then, electric energy produced at turbine-generator system will be E=0.95, E=1.00, E=0.98, and E=0.88 respectively. R. Dipippo (2008) shows similar results.

We assume typical values for the other factors as follows.

Condenser temperature(T_{cd}) : 40.0 ºC (a typical temperature of condenser)

The results are shown in Figure-2. It confirms that the ζ can be expressed as functions of the reservoir temperate (T_r). The form of the approximation equation is given below.

$$\zeta = 0.0000000127T_r^3 - 0.0000124900T_r^2 + 0.0046543806T_r - 0.4591082158 \quad [\text{-}] \tag{21}$$

The curve of the equation (21) is shown in the Figure-2. It shows the available heat function ζ will be zero when the reservoir temperature equals to the separator temperature T_{sp} (151.8 ºC). At this state, the recovered fluid no longer flashes in the separator. This temperature shall be "the plant minimum operation temperature" for a flash type system, that is defined only by separator temperature. Note this should be differentiated from "cut-off temperature" that should define the spatial outer limits of the reservoir

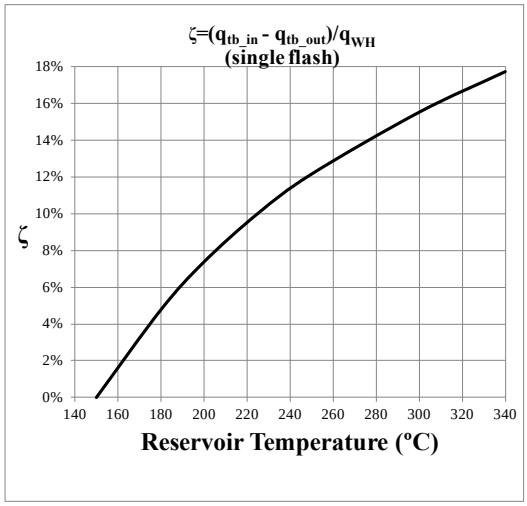

Figure 2: Calculation results of ζ against various reservoir temperatures..

3.3 Selection of Conversion Factor – Turbine-generator efficiency: Exergy Efficiency (η_{ex})

We have started the electric capacity calculation with the equation (7). The coefficient η_{ex} should therefore be defined as:

$$\eta_{ex} = \{E(FL)\} / \{m_{tb_{in}} (h_{tbin} - h_{tbout})\} \quad [\text{-}] \tag{22}$$

Note that this coefficient η_{ex} is the "functional exergy efficiency (DiPippo 2008, p 240)" that is different from both the "utilization factor η_u" defined in the equation (5) of the USGS method and the "conversion factor η_c" in the equation (6) of the prevailing method; the "utilization factor" will include the energy ratio of steam separated from the fluid and exergy efficiency; the "conversion factor" may include the energy ratio of steam separated from the fluid, Carnot efficiency and exergy efficiency (the "conversion factor" of the prevailing method is not necessarily clearly defined, because the method appears not to be explainable from thermodynamic point of view.)

For the parameters in the right side of the equation (22), we examined the 189 existing geothermal power stations all over the world which are listed in the booklet (ENAA 2013 in Japanese), thereafter, we calculated each exergy efficiency defined by the equation (22). In the calculation, steam dryness was also considered immediately after the turbine. After the calculation, we examined the correlation between the exergy efficiencies and the temperature drops $(T_{tbin} - T_{cd})$ between turbine inlet and condenser. Thereby, we obtained the following approximation equation.

$$\eta_{ex} = 0.163897 \ln(T_{tbin} - T_{cd}) - 0.001766 \pm 0.05 \quad [\text{-}] \tag{23}$$

Where $T_{tb\,in}$ is temperature of turbine inlet and T_{cd} is temperature of condenser.

The graphical scatter plot showed large variations; we, therefore, added a distribution range of ± 0.05. This is because the actual efficiencies of turbine-generator system depend on many factors that include the efficiency of basic power plant design, resource temperature, concentrations of dissolved gases in the reservoir fluid, the condition of plant maintenance and so on. Nevertheless and for that reason, the approximation equation (22) reflects actual conditions and therefore applicable for the calculation of the volumetric method.

For our case of $T_{tb_{in}}$ = 151.8 ºC, T_{cd} = 40 ºC,

$$\eta_{ex} = 0.77 \pm 0.05 \quad [\text{-}] \quad (24)$$

3.3 About Recovery Factor R_g

There are a number of references that discussed on the recovery factor. M. A. Grant (2014) recently pointed out that the past values of recovery factor have been in all cases high in comparison with actual performance. We herein refer to some of the papers we examined.

GeothermEx (2004) describes: "Based on our assessment of more than 100 geothermal energy sites around the world, we have found it more realistic to apply a recovery factor in the range of 0.05 (Min) to 0.2 (Max) without application of a most-likely value".

C.F.Williams et al (USGS open-file Report 2008-1296) describes that the recovery factor "R_g for fracture-dominated reservoirs is estimated to range from 0.08 to 0.2, with a uniform probability over the entire range. For sediment-hosted reservoirs this range is increased from 0.1 to 0.25".

S.K. Garg and J. Combs (2010) describes: "Prior to geothermal energy well drilling and testing, it will not in general be possible to obtain any reliable estimates of reservoir thickness and thermal recovery factor. Since it may eventually prove impossible to produce fluid from a geothermal energy reservoir, the possibility of the thermal recovery factor being zero cannot be discounted during the exploration phase; therefore, the proper range for thermal recovery factor is from 0 to 0.20 (the latter value is believed to be the maximum credible value based on world-wide experience with production from liquid-dominated reservoirs)".

AGEA compiled by J. Lawless (2010) describes: "In fracture dominated reservoirs where there is insufficient information to accurately characterize the fracture spacing, adopt the mean USGS value of 14%, or 8 to 20 % with a uniform probability over the entire range when used in probabilistic estimates". "In sedimentary reservoirs or porous volcanic-hosted reservoirs, of 'moderate' porosity (less than 7% on average), adopt the mean USGS value of 17.5%, or 10 to 25% with a uniform probability over the entire range when used in probabilistic estimate". "In the case of sedimentary or porous volcanic-hosted reservoir of exceptionally high average porosity (over 7%), adopt the empirical criterion of recovery factor 2.5 times the porosity to a maximum of 50%".

M.A. Grant (2014) pointed out that there are a wide range of recovery factors: 3-17 % covers the entire range of observed results. This indicates that any result is subject to an error of at least a factor of 2, or alternatively ± 70%. One conclusion is immediate: past recovery factors have been too high, and comparison with actual performance show that an average value of 10% should be used.

The decision on what values should be chosen is left to professionals in charge, that depends on the site conditions, past experiences and/or degrees of diagnostic confidence. Note that the proposed method enables that the recovery factor can be determined independently from both the liquid-steam separation process and conversion process of thermal energy to electric energy.

4. EXAMINATIONS OF THE RESULTS

We calculated electric powers per km^2 (power density) by three different methods of the USGS method, the proposed method and the prevailing method for a comparison purpose with the following parameters.

C_r	= 1.0	[kJ/(kg ºC)]
ρ_r	= 2750	[kg/m^3]
C_f	= 5.0	[kJ/(kg ºC)]
ρ_f	= 790	[kg/m^3]
V	= 2	[km^3], (Reservoir thickness 2 k m)
F	= 0.9	[-]
L	= 30	[years to be converted to second when applied]
R_g	= 0.12	[-]
T_{ref}	= 0.01 ºC (h_L=0 kJ/kg for the proposed method assuming all the recovered heat is sent to the separator)	
	= 20 ºC for the USGS method;	
	= 150 ºC or 180 ºC for the prevailing method	
T_0	= 40 ºC for the USGS method (condenser temperature)	
Conversion factor	η_C	= 0.13 for the prevailing method
Utilization factor	η_U	= 0.45 for the USGS method
Exergy efficiency	η_{ex}	= 0.77 for the proposed method

The results are given in Figure-3. It shows that the proposed method is in good agreement with the USGS method. In addition, it gives similar results to the power density ('the main sequence') presented by wilmarth et al (2014). A deviation from the USGS method is observed at lower side of reservoir temperature. This is because that the USGS method adopts a fixed utilization factor; whereas the

proposed method adopts 'the available thermal energy function" that is a function of T_r as shown in Figure-2. This suggests that the utilization factor may have to be smaller than 0.45 when reservoir temperature is lower, though its impact will be negligible.

On the other hand, the Figure-3 shows that the prevailing method is considerably different from both of the proposed method and USGS method.

We calculated the electric capacity by the proposed method, for the four cases of recovery factors of R_g =0.08, 0.12, 0.15, and 0.20. The other parameters remain same as above. The results are shown in Figure-4. It demonstrates that selection of the recovery factor will give a significant impact on the calculation results of electric capacity estimation by the volumetric method. Similarly, the other underground-related factors ρC, T_r and/or V will have similar impacts on the calculation; which must be emphasized.

From the above and since we have defined the aboveground-related key parameters, the significant differences between the prevailing method and the proposed method shown in Figure-3 may be attributed to the definition differences of the underground-related parameters. This is further discussed in the section 6 Discussion of this paper.

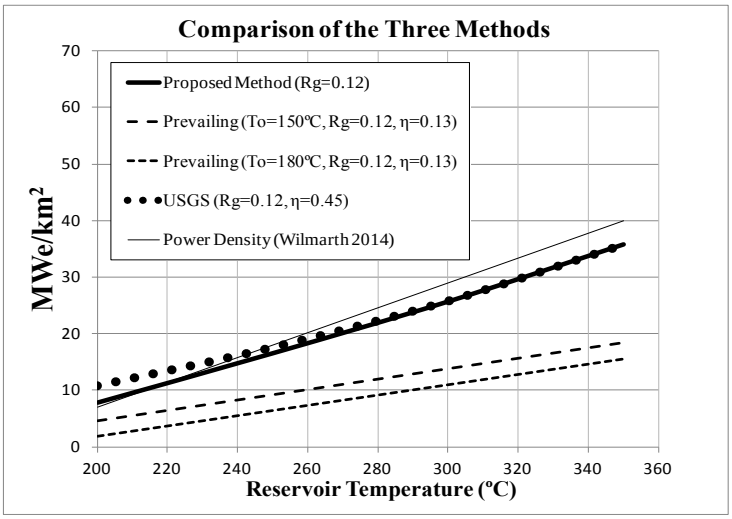

Figure 3: A Comparison of calculated electric power among three methods (Single Flash Power Cycle)

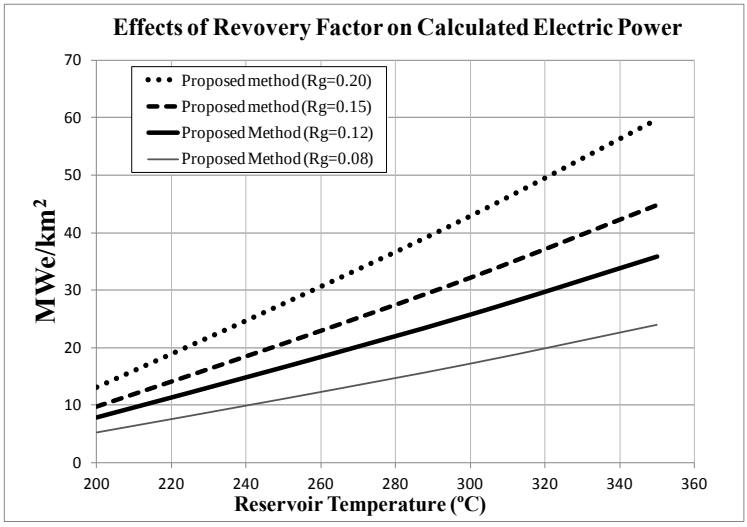

Figure 4: Effects of Recovery Factor on Calculated Electric Power (Single Flash Power Cycle)

5. SUMMARY

We proposed herein a rational and practical calculation approach of the volumetric method by introducing 'the available thermal energy function ζ. The introduction of the available thermal energy function ζ enables us to include the steam-liquid separation process in the

calculation equations rationally, which further enables us to examine the underground-related parameters separately and independently from the aboveground-related parameters; i.e the recovery factor and turbine-generator efficiency (exergy efficiency) can be selected independently, without consideration on steam-liquid separation process; thereby, the proposed method realizes rational and practical calculations of geothermal resources of liquid dominant geothermal field; that can used with the Monte Carlo method.

We hereunder summarize the proposed method for a practical use. Assuming saturated single phase geothermal liquid of temperature T_r ºC at wellhead, T_{sp}=151.8 ºC, and T_{cd} =40 ºC, the following equations for the volumetric method will give an estimation result of electricity capacity of a liquid dominant geothermal reservoir if the underground-related parameters are properly selected.

$$E = \eta_{ex}\zeta R_g \rho C V (T_r - T_{ref}) \big/ (FL) \quad \text{[kW]} \quad (25)$$

where

$$\rho C = (1-\varphi)C_r\rho_r + \varphi C_f \rho_f \quad \text{[kJ/(m}^3\,\text{ºC)]} \quad (26)$$

$$\zeta = 0.0000000127T_r^3 - 0.0000124900T_r^2 + 0.0046543806T_r - 0.4591082158 \quad \textbf{[-]} \quad (27)$$

T_{ref} =0.01 [ºC] (28)

$\eta_{ex} = 0.77 \pm 0.05$ [-] (29)

$R_g = 0.05 - 0.2$ proposed by GeothermEx 2004), [-] (30)

or $R_g = 0.08 - 0.2$ or $R_g = 0.1 - 0.25$ proposed by C.F.Williams (2008),

or $R_g = 0 - 0.2$ proposed by S.K. Garg et al (2010)

or $R_g = 0.05 - 0.2$ or $R_g = 0.10 - 0.25$, or R_g =2.5 times the porosity to a maximum 50%, proposed by AGEA (2010).

or $R_g = 0.03 - 0.17$, 0.10 in average proposed by M.A. Grant (2014)

We may adopt different constants for the available thermal energy function ζ and use a different value of η_{ex} when it should become necessary to change, separator temperature and/or condenser temperature. The calculation procedures are given herein the above. Once the equations are given in a spreadsheet, we can examine as many cases as possible about underground related factors together with the Monte Carlo method.

6. DISCUSSIONS

Having summarized the proposed calculation method above, we continue this paper to examine the relationship between the prevailing method and the proposed method. We regard the USGS method ≈ the proposed method in the following discussions, since the theoretical background of the proposed method is almost same, and the both produce similar calculation results,

6.1 Deriving of Approximation Equations of the Proposed Method

Under the conditions of T_{sp}=151.8 ºC and T_{cd}=40 ºC, Figure 3 implies that the variable term $\zeta(T_r - T_{ref})$ in the equation (11) will be a near liner relation with T_r, thus this liner relation is approximated as:

$$\zeta(T_r - T_{ref}) = (0.3312T_r - 51.911) \quad \text{[liner approximation]} \quad \textbf{[ºC]} \quad (31)$$

With the equation (31), the equation (11) becomes;

$$E = \eta_{ex} R_g \rho C V (0.3312T_r - 51.911) \big/ (FL) \quad \text{[KW]} \quad (32)$$

This is further reduced as;

$$E = (0.77 \pm 0.05) R_g \rho C V (0.3312T_r - 51.911) \big/ (FL)$$

$$E = 0.3312\,(0.77 \pm 0.05) R_g \rho C V (T_r - 157) \big/ (FL)$$

$$E = (0.26 \pm 0.02) R_g \rho C V (T_r - 157) \big/ (FL) \quad \text{[KW]} \quad (33)$$

The equation (33) shows that the equation (11) of the proposed method has eventually become the same equation form as the equation (6) of the prevailing method. Note that the second constant 157 should be the T_{sp} (151.8 ºC) as shown in the previous section 3.2.3; the constant 157 here is the one that resulted from the linear approximation shown in the equation (31).

6.2 Discussions on the Approximation Equation of the Proposed Method in connection with the prevailing method

As the conclusion, two constants of the equation (33) are mere the products of the linear approximation, therefore, any discussions on the equation (33) relating with resource estimations would appear to be meaningless or misleading. However, step-by-step discussions would be helpful to reach this conclusion for future possible discussions that may be instigated; thereafter we will discuss on possible reasons of the differences between the prevailing method and the USGS method.

6.2.1 Is the second constant 157 the cut-off temperature?

A number of constants have been proposed for the equation (6) of the prevailing method in various references. The constants in the equation (33) might be considered to be a variety of the equation (6) of the prevailing method. Here are our observations on the equation (33) in connection with the prevailing method.

a. The approximation constant 157 in equation (33) appears to be the one that is sometimes named as "cut-off temperature". However, this has to be named as the "plant minimum operation temperature", at which the fluid no longer flashes in separator of the assumed separator temperature (151.8 ºC) as described in the previous section 3.2.3. The "plant minimum operation temperature" is rather a "plant-related temperature" that shall be differentiated from the "cut-off temperature". The cut-off temperature is defined as "the temperature below which there is no economic value in the fluid - the temperature at which wells cease to flow or it becomes uneconomic to pump them. This defines the outer limits of the resource (M A Grant, *et al* 2011, p 47)." Thus, the cut-off temperature is a "reservoir related temperature". The plant minimum operation temperature shall not be larger or preferably sufficiently lower than the reservoir related cut-off temperature to ensure fluid to flash in the separator. From this point, the approximation constant 157 in the equation (33) shall not be replaced with reservoir-related cut-off temperature that has to be separately decided from field observations. (If the separator temperature should be designed at 180 ºC for an instance, then the second constant in the equation (33) will be 180; however, the first constant has to be changed in accordance to the calculation and approximation shown above.)

b. As mentioned before, such explanation that the cut-off temperature is included in the equation to exclude fluid of no-economic value from the already defined reservoir seems to be illogical and unexplainable. The inevitable possibility that drilling wells may fail to produce useful fluid from the reservoir shall be dealt with the recovery factor or probabilistic approaches.

c. In addition, the cut-off temperature (= T_{ref}) in the prevailing method is commented by M.A. Grant (2014) in such a context that "the different approaches also implies unrecognized assumptions about the physical process controlling reservoir depletion". The "different approaches" here means the ones that assign a cut-off temperature to T_{ref}, that are derived from the Icelandic practice. Our observation on the unrecognized assumptions is that such physical process controlling reservoir depletion seems not to be a matter of T_{ref} to be expressed in the thermodynamic equation. If the temperature of a part of the reservoir is expected to fall down below the cut-off temperature during operation period, it seems to be logical to reduce the value of either the reservoir volume or the recovery factor, or the plant life time for an extreme case.

6.2.2 Is the second constant 157 the reference temperature for the power generation cycle?

a. On the other hand, from a thermodynamics point of view, the equation (33) could possibly be interpreted in such a way that the power capacity *E* calculated is an energy fraction converted from the recovered heat energy when the temperature changes from T_r to 157 ºC, with adjustment by the multiplier (0.26 ± 0.02) and the divisor (*FL*). In this context, the approximation constant 157 in the equation (33) is the one that is named as "reference temperature", "rejection temperature", "base temperature" or the like; the temperature in the equation (33) shall be defined as the temperature of the final state of the fluid at a point of a power plant. However, this corresponds to the rejection temperature at the separator, not the final state temperature of the whole power generation cycle as seen above. This constant shall not be regarded as the final state temperature of the power cycle. At the same time, the first constant (0.26 ± 0.02) shall not be defined as a kind of a logically-derived efficiency, though it looks seemingly to be a meaningful coefficient.

6.2.3 What are the fist and the second constants in the equation (33)?

Consequently, we have to come back to the equation (33); whereat, we recall that the both constants 157 and (0.26 ± 0.02) were the mere resultants of the linear approximation. They were derived as the impartible combination under the specific assumptions (T_{sp}=151.8 ºC and T_{cd}=40 ºC). Any of these two constants shall not be examined independently or shall not be changed separately. Those two approximation constants, as it were, are "the virtual reference temperature" and "the virtual conversion factor" of "the virtual geothermal power plant" that is virtualized on the basis of the approximation equation (33), that has been derived through the series of calculations, that does not represent the thermodynamic process of any actual power plant. Thus, discussions on these approximation constants will probably be meaningless and possibly be misleading or even harmful when geothermal resource is estimated by the volumetric method.

6.3 Discussions on the Relation between the Prevailing Method and the USGS Method (≈the Proposed Method)

a. Nevertheless, the equation (33) is simple in form, not many variables included, and thus easy to use with Monte Carlo simulation. The prevailing method appears to have been used by adopting approximate a half value of the first approximation constant (0.26 ± 0.02) and a cut-off temperature similar to the second approximation constant 157 to suit field conditions. Although these constants shall not be allowed to use from the thermodynamic point of view, estimations by the prevailing method have been reported to be in accordance with other more precise estimation methods or field observations (Sarmiento et al 2007, which practices the prevailing method, but appears to have referred to Muffler P., et al (1978) of the USGS method as the methodological base. Similar undistinguishing quotations are seen in other references).

b. At the same time and on the other hand, the USGS method (≈ the proposed method) has been used for resource estimations, although the USGS method gives larger results than the ones of the prevailing method when the same underground-related parameters are given to the both methods as shown in Figure -3. Our observations are as follows.

(i) We have defined the aboveground-related parameters for the proposed method (≈ the USGS method), thus the discrepancy may possibly be due to differences of interpretations on underground-related parameters; i.e. for the resource estimation of the same geothermal field, the practitioners of the prevailing method would propose the $(R_g\rho CV)_{prevailing}$ as their underground-related parameters; whereas the other practitioners of the USGS method (≈ the proposed method) would propose the different parameters $(R_g\rho CV)_{USGS}$; $(R_g\rho CV)_{prevailing} \neq (R_g\rho CV)_{USGS}$.

(ii) The USGS method appears to assume that the all the heat energy relating to $(R_g\rho CV)_{USGS}$ should be extracted at the ground surface, because the method (when R_g=0.12 in Figure 3) gives similar results to the "main sequence" of the power density (Wilmarth *et al*., 2014); the analysis of the power density does not include the information of failed wells. In other words, possibility of well failures may not be included in the USGS method. Geothermal wells however are not always successful to produce useful fluid. Sanyal S.K *et al*. (2012) analyzed 2,528 geothermal wells in 52 field in 14 countries and found that the mean success rate was 68%. At early stages of exploitation the rate varies in a range from 20% to 60 % approximately. If the average drilling success rate should be considered for a resource estimation, the resultant recovery factor would be R_g=0.12 x 68%= 0.08; with this R_g=0.08 the USGS method will come close to the prevailing method of T_0=150 ºC as shown in Figure-4. M.A. Grant (2014) strongly pointed out the past values of R_g have been all cases too high, an average value of R_g=0.10 should be used.

(iii) On the other hand, the prevailing method even with R_g=0.25 is reported to be in good agreement with actual performance (Sarmiento et al 2007). Thus, it may allow localized non-productive zones to be included within the reservoir, by adopting amended constants to the places of the first and second constants of the equation (33) "to calibrate" the results to the actual performance. However, again, it shall not be the constants of the equation (33) but the underground-related parameters such as R_g, V and/or others that shall be examined. In other words, the calculation form of the equation (33) may have falsely diverted our attentions from the underground-related parameters to the aboveground-related parameters or the approximation constants in the approximation equations.

6.4 Closing discussion

(i) All those may be resultants from usage of ambiguously defined parameters, which may has allowed practitioners to adopt various values of not only underground-related parameters (R_g, ρC, V, *cut-off temperature*) but also aboveground-related parameters (T_{ref}, T_{sp}, T_{cd}), with considerations on relations with others as if some of those would be functions of others; such considerations however may sometimes not be necessary if the parameters used should be well-defined.

(ii) Instead, we have introduced the equation (11) with clear definitions of the aboveground-related key parameters, including the flashing process with the typical condenser conditions. The proposed method could allow us to examine the underground-related parameters rationally, being independent from considerations of relations with aboveground-related parameters. The proposed method will also allow us to avoid possible misleading that may be caused by the prevailing method in the form of the equation (33).

(iii) In any cases, it is of paramount importance to use the volumetric method with very careful and prudent examinations and considerations together with clear definitions on the underground-related parameters.

7. CONCLUSION

The USGS method is theoretical, but practice with the equations together with Monte Carlo method seems to be laborious; the prevailing method is somewhat questionable from theoretical point of view. We have herein proposed a rational and practical calculation method for volumetric method for a specific but typical case. We would like to recommend to use the equation (25) because the proposed method enables us to assess electrical capacity by clearly and rationally defined parameters for the equations; thereby we could examine the underground-related parameters, resulting in clearer understandings of the electrical capacity estimation of a geothermal reservoir. Once clearer assessment with the specific but typical conditions of the aboveground parameters has been made, one could extend assessments with other conditions of the aboveground parameters for comparisons. If the aboveground-related parameters T_{sp} and/or T_{cd} should be changed to suit a particular field condition, we could modify the constants of the available energy function.

We have also derived the simplified equation (33) that appears to be the same form of the prevailing method and provides us with a simple calculation procedure. It however masks its theoretical background completely, which may hinder us from proper and deeper understanding of underground related parameters to be used for the volumetric estimation. This may mislead us to unnecessary considerations and/or discussions on the virtual "conversion factor" and/or virtual "reference temperature" of the "virtual power plant" virtualized by the equation (33). We therefore would like to recommend to avoid using this equation (33).

Finally, very careful and prudent examinations and considerations shall be required for determination of underground-related factors, in particular R_g and/or V. If estimation results by the proposed method should not be in accordance with other more precise estimation methods or field monitoring results, the underground related parameters have to be examined. Well drilling success rate could be in cooperated when we determine R_g and/or V.

ACKNOWLEDGMENTS

We would like to express our greatest appreciation to Tsuneo Ishido, Daisuke Fukuda, Mineyuki Hanano, Katsuya Kuge and Mayumi Hayashi for helpful discussions and suggestions; Steinar Þór Guðlaugsson, Helga Tulinius and Benedikt Steingrímsson for their

comprehensive comments on a drafted paper; and following eminent professionals Jim Lawless, Sabodh K. Garg and Hirofumi Muraoka for kind e-mail communications. We also would like to express our gratitude to our colleagues working together for helpful discussions as well as Nippon Koei Co., Ltd for supporting us to complete this work.

REFERENCES

AGEG-Australian Geothermal Energy Group Geothermal Code Committee. *Geothermal Lexicon For Resources and Reserves Definition and Reporting Edition 2, compiled by J. Lawless*. Australia: AGRCC-The Australian Geothermal Reporting Code Committee, November 2010.

Brook, C.A., Mariner, R.H., Mabey, D.R., Swanson, J.R., Guffanti, M. and Muffler, L.J.P. *Hydrothermal Conversion Systems with Reservoir Temperature >90ºC: in Assessment of Geothermal Resources of the United States – 1978, L.J.P. Muffler, editor, U.S. Geological Survey Circular,*. Arlington,VA, US: USGS, 1978.

DiPippo, Ronald. *Geothermal Power Plants; Principles, Applications, Case Studies and Environmental Impact, 2nd edition*. Oxford, UK: Elsevier, 2008.

ENAA: Engineering Advncement Association of Japan. *Study on Small Scale Geothermal Power Generation and Cascade Use of Geothermal Energy (in Japanese)*. Tokyo, Japan: Japan Oil Gas and Metals Nationla Corporation, 2013.

ESMAP (Energy Sectore Management Assistance Program, World Bank). *Geothermal handbook: Planning and Financing Power Generation*. Washington, USA: International Bank for Reconstruction and Development, 2012.

Garg, Sabodh K. *Appropriate Use of USGS Volumetric "Heat in Place"Method and Monte Carlo Calculations*. Stanford, CA, U.S: Proceedings, Thirty-Fourth Workshop on Geothermal Reservoir Engineering, Stanford University, 2010.

Garg, Sabodh, K. and Jim Combs. *A Reexamination of USGS Volumetric "Heat in Place" Method*. Stanford, CA, USA: Proceedings, 36th Workshop on Geothermal Reservoir Engineering, Stanford University, 2011.

GeothermEx. *New Geothermal Site Identification and Qualification*. California: California Energy Commission, Public Interest Energy Reserch Program, 2004.

Grant, M. A and P, F. Bixley. *Geothermal Reservoir Engineering second Edition*. Oxford, UK, 359p: ELSEVIER, 2011.

Grant, M. A. *Stored-heat assessments: a review in the light of field experience*. Geothe. Energy. Sci,. 2, 49-54, 2014. Germany: Geothermal Energy Science, 2014.

Muffler P., Cataldi R. *Methods for Regional Assessment of Geothermal Resources*. Great Britain: Geothermics., Vol. 7. pp. 53-89, Pergamon Press Ltd, 1978.

Muffler, L. J. P.; Editor. *Assessment of Geothermal Resources of the United States - 1978; Geological Survey Circular 790*. USA: USGS, 1978.

Pálmason, G., Johsen, G. V., Torfaxon, H., Sæmundsson, Ragnars, K, Haraldson, G.I., and Halldórsson, G.K. *Mat á Jarðvarma Íslands (Assessment of Icelandic Geothermal Resources) (in Icelandic)*. Report OS-85076/JHD-10,. Reykjavik, Iceland: Orkustofnun Jarðhitadeild (Iceland Energy Authority, Geothermal Division), 1985.

Sanyal, S. *Success and the Leaning Curve Effect in Geothermal WEll Drilling - a Worldwide Survey*. Proceedings of the 37th Workshop in Geothermal Reservoir Engineering,. Stanford, CA, USA: Stanford University, 2012.

Sarmiento, Z. F, Bjormsson, G. *Reliability of early modeling studies fr high-temperature resevoirs in Iceland ad The Philippienes*. Proceedings, 32nd Workshop on Geothermal Reservoir Engineering. Stanford, CA, US: Stanford University, 2007.

Subir, Sanyal K.; Sarmiento, Zosimo. "Booking Geothermal Energy Reserves." GRC Transactiions, vol. 29. 2005.

Wiliams, C. F. *Development of Revised Techniques for Assessing Geothermal Resources*. Stanford, California, USA: Proceedings, 29th Workshop on Geothermal Reservior Engineering, Stanford Univ., 2002.

Williams, Colin F., Marshall J. Reed and Robert H. Mariner. *A Review of Methods Apllied by the U.S. Geological Survey in the Assessment of Identified Geothermal Resources*. USA: Open-FileReport 2008-1296, U.S. DEpartment of the Interior, U.S. Geological Survey, 2008.

Wilmarth, Maxwell and James Stimac. *Worldwide Power Density*. Stanford, CA, USA: Proceedings, Thirth-Ninth Workshop on Geothermal Reservoir Engineering, Stanford Unversity, 2014.

EoD

Appendix-7 Output of Meeting

Data Collection Survey for Geothermal Development in Republic of Djibouti (Geophysical Survey)

Minutes of Workshop

Place: Palais du Peuple, Djibouti

Date: August/10/2015, 9:00-11:00

Attachment: 1. Agenda of the Workshop
2. Handout material
3. Participants list

The Workshop

1. The ODDEG moderator (Hamoud Souleiman) introduced the Workshop.
2. Mr. Sassadate, the representative of JICA Djibouti office welcomed all the participants and described the geothermal development cooperation between Djibouti-Japan.
3. Mr. Abdou Mohamed Houmed, Director General of ODDEG, expressed gratitude for the assistance in geothermal development extended by the government of Japan and JICA and made his opening address to the participants.
4. Followed by the invitation to the presentation of the survey results, Mr. TAKAHASHI, the Team Leader, and Mr. TAKEDA, the geophysicist of the JICA Survey Team made the presentation in accordance to the handout material attached hereto.
5. The Question and Answer session followed; the minutes of the questions and answers are as follows.

Q&A:

- Q 1: With no clear cap rock structure observed in resistivity results, how the aerial limitation of the geothermal reservoir was decided ?
  - A: The JICA team assumed that the reservoir could exist in the portion of in 40 – 160 Ωm approximately in the plateau areas, based on the correlation between the resistivity distribution and the depth of clay minerals in a past well (Hanle-2). The western boundary of the reservoir was assumed to be the main fault delineating the plateau and the plan; the northwest boundary is correspondent to the limit of the survey area; although all those are preliminary.
- Q 2. The TEM data was used only for the static shift correction. Why did you not analyze the resistivity structure of shallow part (shallower than 300m) despite that the TEM data in shallow area were obtained.
  - A: It was not analyzed, because the target of this survey is geothermal structure in deep

area . Our effort was concentrated on the purpose we should attain.

- ✧ Q 3: Is the deep high resistivity area not corresponded to the cold area? If that is the heat source, cap rock structure would have been created above that area, and it appears in resistivity structure.
  - ➢ A: The fact that the plain area is cold was verified by the past survey. The fumaroles that are observed on the plateau area imply that there should be the heat source under the ground nearby. We assumed the heat source should be corresponded to the high resistivity zone in plateau area.
- ✧ Q 4: Will a correlation be conducted between the depth of alteration mineral, resistivity value, and the temperature log? It will help you to understand geothermal structure.
  - ➢ A: It is of course carried out in the future test well drilling.
- ✧ Q 5. The main fault on the SW side should incline to NE direction instead SW direction according to field observation.
  - ➢ A: All the information we have not only from desk top work but also field observation the fault on the subject shall be interpreted to incline to SE side. The geological map ORSTOM (1987) shows the similar cross section.
- ✧ Q 6. There will be no heat in the plateau unless there should be not dome structure. The heat source in the Hanle Plateau should be structural origin.
  - ➢ A: There are a number of volcanic corn on top of the Plateau, which implies a recent volcanic activities. Fumaroles are associated with Rhyolite dyke/vain in many cases. It would be reasonable that the heat could be associated with those volcanic activities.
- ✧ Q 7. Correlation between the MT survey and the geological logs of the past well will be useful to understand the geological structures or setting in Hanle.
  - ➢ A: The consultant tried such correlation during this analysis period; but, could not get useful results because all geology in the all past wells were classified as basalt. It was not possible to interpret resistivity of rock from the borehole logs. It is also not possible to correlate the MT resistivity with thin changes of rock faces/characteristics

    In Hanle plain, the alluvial sediment is about 100 m deep. This is not a target of the MT survey for the geothermal development.
- ✧ Q 8. Was the geothermal reservoir model created by all the geology, geochemistry and geophysical data being put together for consideration? There are much information in Hanle, conducted by Italian consultants in 1980's.
  - ➢ A: All and as much information as possible we have at hand were all integrated for the construction of the geothermal reservoir.
- ✧ Q 9. Subsurface temperature measurement was very successful in Lac Abe. The additional survey shall include the sub-surface temperature. Measurement in depths (30-50 cm deep) will

work well if measurement is carried out in night. If JICA provides the ODDEG with equipment, which are not expensive, the ODDEG could do the survey by themselves.

- A: The consultant appreciate the proposal and the consultants consider it useful. But, according to a literature the thermo-sensor shall be put in to the ground down to 2 m to avoid the influence by the air temperature, but the Hale Plateau is so rocky that thermo-sensor could not be penetrated in to 2 m depth. This is the reason why the consultant did not propose the subsurface temperature measurement in Hanle. However, we could propose JICA head office to procure tools and equipment for the survey by which the ODDEG would do the survey since those are not expensive.

- Q 10. With the additional survey proposed by the Consultant, could it be possible to reach a decision whether test well drilling is to be proposed or not.
  - A: It will depend on the results to be obtained. The consultant shall be in a position who shall provide a clear proposal on the decision of test well drilling.

Through the above technical discussions, it was generally agreed that the proposed additional surface survey would be necessary before the test drilling program.

Finally the consultant requested comments on the Draft Final Report to be sent to the Consultant through ODDEG by 24th August 2015.

The work shop was closed.

** End of Document **

Confirmed by:

OFFICE DE DEVELOPPEMENT DE L'ENERGIE GEOTHERMIQUE
Le Directeur Général
Abdou Mohamed Houmed
ODDEG

Abdou Mohamed Houmed
Director General, ODDEG

Shinya Takahashi
Team Leader, JICA Survey Team

République de Djibouti
Unité – Egalité – Paix

OFFICE DJIBOUTIEN DE DEVELOPPEMENT DE L'ENERGIE GEOTHERMIQUE

(ODDEG)

DATA COLLECTION SURVEY ON GEOTHERMAL DEVELOPMENT IN DJIBOUTI
DRAFT FINAL REPORT

Geophysical Survey in Hanlé Garabbayis

REMARKS AND COMMENTS OF THE DRAFT FINAL REPORT

Made by ODDEG team

With response from the JICA Team

August, 2015

Sublimated to the quality of work of this scientific exercise, We would like to congratulate all the experts of the mission of JICA for the professionalism and precision of this work done with heart and commitment.

The ODDEG's officers have edited some comments which have been summarized below. The remarks and comments can be divided in two main parts. The first part concerns the form of the report and the second part is focused on the content and the technical matters.

1st Remark:

In the cover page and figure 2.5: There is confusion over the drilling location: Hanlé Garabbayis 2 and 2 have been interchanged.

It will be corrected, thank you.

2nd remark:

In paragraph 2.4.2 you mention figure 2.9, but this figure is missing

This will be corrected, thank you.

3rd remark:

Table 2.2: Well Garabbayis 1 is drilled by Djiboutian institution named Genie rural now called Direction de l'eau. It is not drilled by GENZL.

Thank you for your information.

4th remark:

The TEM data was used only for the static shift correction. Why did you not analyze the resistivity structure of shallow part despite that the TEM data in shallow area were obtained?

The subject for interests lies in the deeper part, i.e. approximately 500 m or more, in case for geothermal exploration. The deeper part is explored by MT survey rather than TEM survey. We, therefore, usually use the TEM data only for static shift correction when we conduct MT survey. For this reason, TEM survey plan is made to acquire information up to approximately 500 m, i.e. e-current intensity to be used is decided based on this requirement.

You mention "Layered resistivity structures which show the resistivity variation of high-low-high from surface to deep zone were obtained at almost all stations.'' This is another reason to focalize for TEM.

The high-low-high resistivity structure from the TEM results is within the range of the results of the MT-survey in the range of the depth. The high-low-high structure within 500 m depth will hardly affect the overall interpretation of the reservoir resistivity structures. Only a considerably thick low resistivity cover could be interpreted as a cap-rock structure. We will do the 1-D analysis using the TEM survey and the results are attached here to. .

On the field, in TEM method, the used configuration was central loop with a loop transmitter 100 x 100m. I think that with this configuration we can imaged easily the first 500 meters or more as we can see on this figure below.

The diffusion depth δ (m) of TEM survey is regarded as a rule of thumb of the exploration depth for TEM method and it is estimated by the following equation.

$$\delta = \sqrt{\frac{2t\rho}{\mu}} = (2*0.02*10/1.257*10^{-6})^{0.5} = 564$$

Where, ρ: ground resistivity (ohm-m), t: time after turning off the primary field (sec), μ: magnetic permeability

Because we could acquire good repeatable TEM data till 0.02 sec in this survey, the exploration depth of TEM was around 500 m at most. Due to this reason, the TEM data acquired by this survey can be used upto 500 m deep. We believe that analysis for more than 500 m will be misleading.

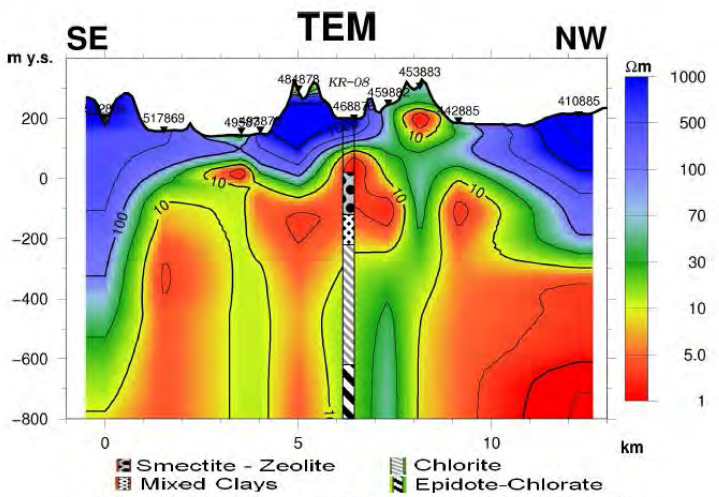

FIGURE 15: Resistivity cross-section from the 1-D inversion of TEM soundings, extending down to 800 m b.s.l.

Model obtained by Icelanders with the TEM method on one of their site.

We would like to refrain from any comments on the figure above, because we do not know the survey conditions. One thing we could comment is that the TEM results may be used for area deeper than 500 m if large e-current is applied when measured. This may be done when MT survey is not conducted at the same time.

We have interpreted the MT data from 4 profiles (HNL100 -HNL400) with a 1D approach. The 1D resistivity models obtained are interpolated as profile and we observe the following sequence: high-low-high as we can see on these following figures.

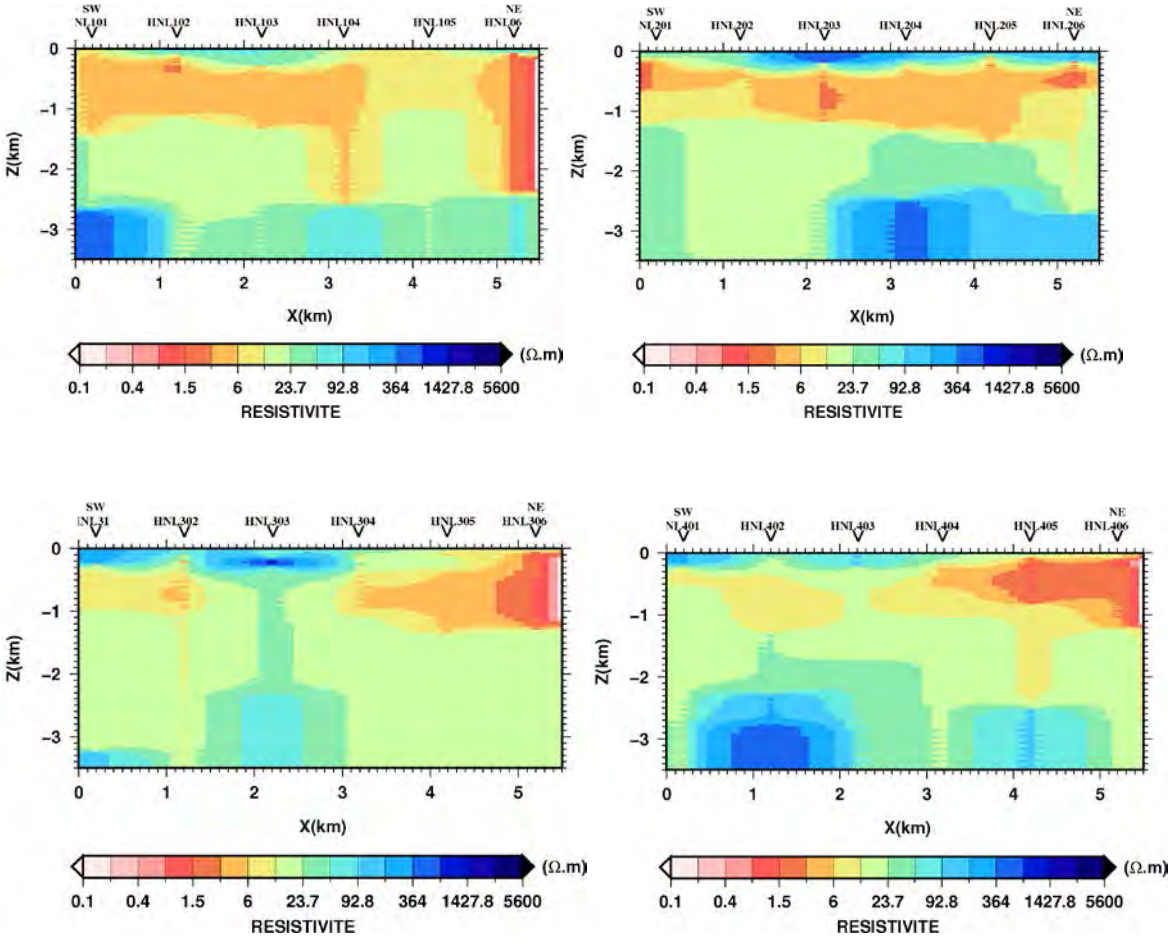

Your geophysical report also mentions this sequence of resistivity in near surface (models TDEM).

So, according to your study unfortunately there is no correlation between the TDEM models and models MT at least in the near surface part (0-1 Km).

Most of apparent resistivity curves obtained this time show that the two curves xy and yx are more or less consistent in shallower zones (i.e higher frequency parts), which implies that 1-D analysis is applicable. On the other hand, the two apparent resistivity curves are not consistent in deeper zones (i.e. lower frequency parts), which implies that 1-D analysis may not be applicable. From the above principle, we are confident that the 2-D analysis is more suitable for deeper part, while 1-D analysis is applicable for shallower parts. We will make TEM 1- D detail analysis and the results are attached hereto.

5th Remark:

Chapter 9 point 9.2:

- For this sentence: “The Assal Geothermal Project is being handled by the EDD. The ODDEG is not now in charge of the project. Much information therefore is not available”.
  Replace instead by “The Assal Geothermal Project is being handled by the EDD. The ODDEG and CERD serve like a technical support. Much information therefore is not available’’

We will correct it accordingly, thank you.

- Dr. Kayad is a officer in ODDEG not from Ministry of Energy

We will correct it accordingly, thank you.

Chapter 9 Point 9.3

Training in Mai 2015 is postponed in September 2015

We will correct it accordingly, thank you.

6th Remarks:

Chapter 10 Point 10.2:

Instead of PK12, it is PK20

We will correct it accordingly, thank you.

Recommendations

- We want to highlight the time that the environmental survey consume is very high. Our side we do all necessary arrangements to accelerate the procedure, could you make the same from your part?

We will do our best to shorten the time period required.

- For the next survey it is good to add some geological survey like the outcrop. This give a good idea to do the correlation between geophysical case and geological for the subsurface.

We will dispatch a geologist as well. Joint inspection may be proposed if possible.

- The TEM is carried out to have static correction of MT data only. And your target of this survey is geothermal structure in deep area. This was our error for Assal area in the past. We ignored shallow reservoir (190°C at 600-700 m .b.s.l). ODDEG need to take account of this shallow reservoir for interpretations. And it is necessary to interpret the shallow deep less than 800 m by using TEM survey because the central loop by 100x100 can go deeper according the literature.

Thank you for your information on your past experiences.

As we explained above, our TEM survey was designed to use for static correction purposes. Thus, the e-current was selected to collect information from shallower zones. The e-current was not sufficiently large to collect information from area deeper than 500m. Instead, MT survey collect the information from deeper area. A large e-current will be applied to TEM survey only when TM survey is not conducted, as far as we understand.

- And also take account some questions and comments made in the workshop and it is in the minutes of workshop.

Supplemental explanations have been added to the minutes of the work shop

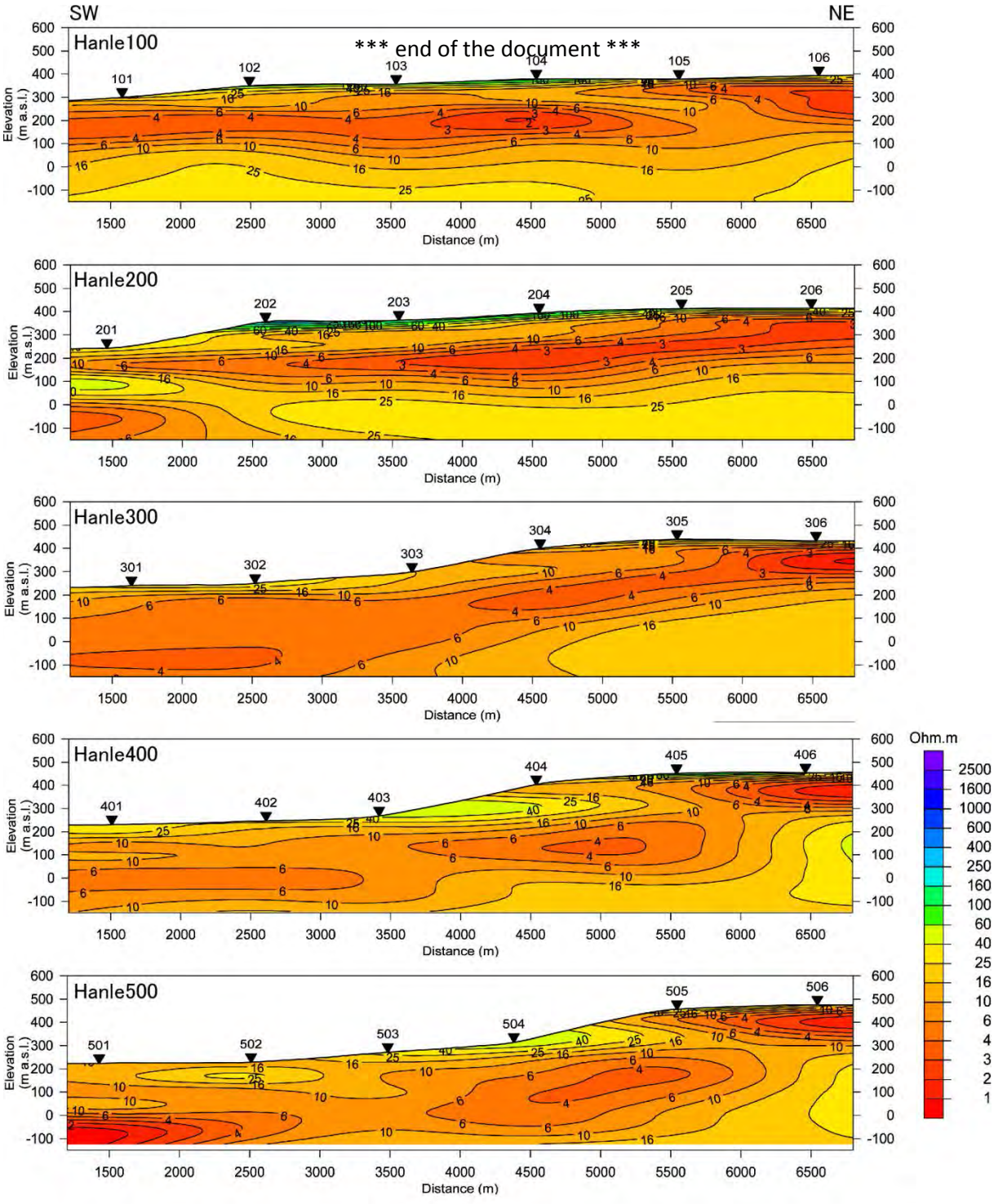

*** end of the document ***

The resistivity cross sections of the very shallow zone from the results of TEM 1D inversion analysis

Memo between the ODDEG and the JICA survey Team

A conversation was made between the Director General of the ODDEG and the Team Leader of the JICA Survey Team after the workshop for the Draft Final Report held on 10th August, 2015. This memo has been prepared to confirm what were talked about between them, in order for the JICA Survey Team to convince the precise message from the ODDEG to JICA head office.

1. The ODDEG recognizes that the geophysical survey in Hanle Garabbayis has revealed that the resistivity pattern is different from the one of the typical pattern in geothermal prospects.
2. With that information, the ODDEG agrees to the recommendations for the additional surface survey presented by the JICA Survey Team in Hanle Garabbayis site.

3. In parallel with the JICA survey in Hanle Garabbayis, the ODDEG intends to conduct gravity survey and supplemental geophysical survey (MT/TEM survey) in Nord Ghoubbet, where the CERD conducted a pre-feasibility study in 2011. The study included geochemical survey and geophysical survey of 30 monitoring points, together with review of existing information on gravity survey, magnet survey conducted by BGR. An additional survey is to be conducted at about 30 points in Nord Ghoubbet by the professionals of the ODDEG.
4. The purpose of the surface survey intended by the ODDEG is to raise Nord Ghoubbet up to a level where a comparison could be made with Hanle Garabbayis site to select a better site for further exploration. This approach is in accordance to the one that was proposed by the Data Collection Survey of JICA in 2014.

5. In this regard of Nord Ghoubbet, the ODDEG wishes the JICA Survey Team to provide its technical assistance for technical guidance on site and for the data analysis possibly conducted in Japan as well.
6. The ODDEG would like to request to JICA to provide an updated software such as WingLink for MT analysis since the ODDEG has only an outdated software for 1-D analysis, so that the ODDEG could conduct review analysis whenever necessary including the data of other sites with the capacity to be enhanced through the technical assistance from Japan. The software could be utilized for other purposes such survey as groundwater or mining resources or etc.

The ODDEG, as the competent organization for geothermal development of the Republic of Djibouti, sincerely wishes to realize the test well drilling program with the technical assistance from JICA.

(10th August, 2015; recorded by the JICA survey team)

Abdou Mohamed Houmed	Shinya Takahashi
Director General, ODDEG	Team Leader, JICA Survey Team